

## LITERATURE REVIEW

# Review of morphing concepts and materials for wind turbine blade applications

Xavier Lachenal, Stephen Daynes and Paul M. Weaver

Department of Aerospace Engineering, University of Bristol, Bristol BS8 1TR, UK

## ABSTRACT

With increasing size of wind turbines, new approaches to load control are required to reduce the stresses in blades. Experimental and numerical studies in the fields of helicopter and wind turbine blade research have shown the potential of shape morphing in reducing blade loads. However, because of the large size of modern wind turbine blades, more similarities can be found with wing morphing research than with helicopter blades. Morphing technologies are currently receiving significant interest from the wind turbine community because of their potential high aerodynamic efficiency, simple construction and low weight. However, for actuator forces to be kept low, a compliant structure is needed. This is in apparent contradiction to the requirement for the blade to be load carrying and stiff. This highlights the key challenge for morphing structures in replacing the stiff and strong design of current blades with more compliant structures. Although not comprehensive, this review gives a concise list of the most relevant concepts for morphing structures and materials that achieve compliant shape adaptation for wind turbine blades. Copyright © 2012 John Wiley & Sons, Ltd.

## KEYWORDS

smart structures; load alleviation; morphing structures; shape adaptation

## Correspondence

Xavier Lachenal, Department of Aerospace Engineering, University of Bristol, Bristol BS8 1TR, UK.  
E-mail: Xavier.Lachenal@bristol.ac.uk

Received 18 February 2011; Revised 9 September 2011; Accepted 14 September 2011

## 1. INTRODUCTION

The main objective of current research and development in the wind turbine field aims at lowering the cost per kilowatt-hour of energy produced, thus partly explaining the drastic increase in size of the wind turbines over the last decade. This growth means higher towers and longer blades to take advantage of the generally faster winds at greater heights, according to Hansen,<sup>1</sup> and of the better energy harvesting capability. This size increase also means higher stresses in the wind turbine components, leading to an increase in control complexity, from stall-regulated fixed pitch rotors in the 1980s to independent control of the blade pitch nowadays. However, with the next generation of wind turbines reaching 160 m in diameter or more, further growth in size requires new approaches to load control. Recent research<sup>2–5</sup> shows significant potential for load reduction by actively adapting the blade profile at any span-wise location in response to the wind environment. Consequently, ‘smart rotor controls’ are currently being investigated. These are often active surfaces distributed along the blade and controlled by measured quantities, able to locally adjust the blade profile and quickly reduce the loads in real time. A number of concepts have been investigated and reported by several laboratories, and many articles can be found in the literature, including those of Buhl *et al.*,<sup>2</sup> Andersen *et al.*<sup>6</sup> and Bak *et al.*<sup>7</sup> Variable geometry ‘morphing’ structures, for their adaptive load-carrying capability, reduced actuation cost and aerodynamic efficiency, are in essence ideal candidates for smart rotor concepts and were initially investigated and employed in helicopter research. In this review, a comparison between wind turbine and helicopter blades is first presented followed by recent concepts employed in the rotorcraft industry. Details of candidate materials for morphing structures are then discussed, and finally, a comprehensive list of structural concepts for wing and blade morphing is provided. It is noted that both passive and active morphing solutions exist for wind turbine blade load alleviation. However, passive morphing is limited to the tailoring of the blade stiffness, as demonstrated by Lobitz *et al.*,<sup>8–10</sup> and/or to the shape of the blade, as detailed in Ashwill *et al.*<sup>11–13</sup> and Zuteck.<sup>14</sup> In this review, only concepts for active morphing are listed with emphasis given to structural shape changes, noting that

a discussion of actuator technology is not the current focus of this article. Significant amounts of literature already exist on actuation aspects of morphing, including the characterisation and usage of smart materials such as those made from piezoelectric, electrostrictive, magnetostrictive and shape memory materials (alloy and foam) or electrorheological fluids. The reader is referred to review articles by Straub<sup>15</sup> and Chopra,<sup>16</sup> Hulskamp<sup>17</sup> or Thill *et al.*<sup>18</sup> for more details.

## 2. HELICOPTER RESEARCH AND DESIGN EXPERIENCE

During the past 20 years, extensive experience has been gained on smart control in the field of helicopter rotor technology, mainly to minimise noise and vibration, resulting in several successful concepts. Straub and Chopra reviewed several ideas for control including pitch, twist, camber and moveable control surfaces.<sup>15,16</sup> Specifically, as shown in Figure 1, active tip, active twist and active flaps were explored, and their load reduction capabilities demonstrated. The active blade tip locally twists, nominally reducing aerodynamic loads and root bending moment. However, the turbulence occurring at the blade tip inherently reduces the benefit of such a device. Chopra<sup>16</sup> did show this concept to be promising as an auxiliary device for partial control of noise and vibration. Active twist continuously varies the angle of attack over the span of the blade and is achieved by embedding smart material into the anisotropic material composing the blade skin. Thus, the entire blade can be twisted without the use of complex mechanisms such as torque rods. Chopra<sup>16</sup> shows potential reduction of up to 10% of the blade's torsional loads. The main advantage is the absence of moving parts whilst maintaining aerodynamic characteristics of the blade. However, it requires considerable changes in the blade structure, resulting in increased weight and decreased stiffness. Finally, active flaps are reported to achieve the best load control of all the concepts currently investigated, with a reduction of 50% to 90% in vibration achieved during the flight of an EC145 helicopter equipped with piezoelectric actuated trailing edge blades, as reported by Dieterich *et al.*<sup>19</sup> and Roth *et al.*<sup>20</sup> However, because of the small strain capacity of smart materials in general, discrete mechanisms and complex internal structures are required to achieve the stroke needed for shape change, with examples given by Chopra.<sup>16</sup> These designs and results are of great interest for wind turbine smart control applications and should be considered when developing new concepts for wind turbines.

However, some differences exist between helicopter and wind turbine applications. Operating parameters differ between the two: helicopter blades are subjected to higher rotational speeds, frequencies, centrifugal forces and aerodynamic forces, whereas wind turbines are larger, more cost driven and not so weight or vibration critical. In both applications, maintenance must be as low as possible, and aero-acoustic noise is a strong consideration. Both applications also face similar challenges in predicting and understanding the unsteady aerodynamic loads and performance, dynamic stresses and aeroelastic

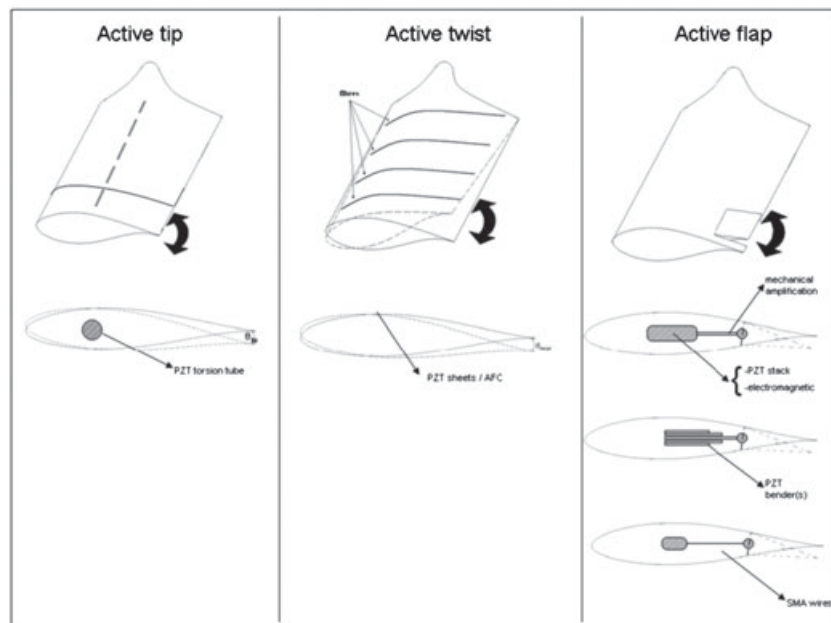


**Figure 1.** Schematic of helicopter main smart blade concepts.<sup>21</sup> PZT, piezoelectric; AFC, active fiber composites; SMA, shape memory alloy.

response of the blade. Whereas helicopter blades see highly periodic aerodynamic loads, wind turbine blades are subjected to complicated effects such as wind shear, turbulence, tower shadow and the wake of other turbines.

### 3. REVIEW OF MATERIALS FOR MORPHING STRUCTURES

Current wind turbine blades are usually made of fibre reinforced plastic (FRP) webs surrounded by two FRP shells acting as aerodynamic fairings. For structural integrity to be maintained and for buckling phenomena to be limited, foam is inserted into the aerofoil's trailing edge, as shown in Figure 2. Whereas most of the torsion, axial and bending loads are counteracted by the box beam (comprising webs and flanges), the blade skin is required to withstand a combination of tensile, compressive and shear forces and transfer the distributed aerodynamic pressure loads to the inner structure.

This design is typical of lightweight structures, which are optimised to be load carrying and stiff, as shown in Figure 3 (Aimmanee *et al.*<sup>22</sup>). When shape adaptation is required, neither conventional or lightweight structures nor compliant mechanisms are optimised for a wind turbine blade. The former are heavy, the latter are not load-carrying, and lightweight structures are too stiff; this is why morphing structures could offer design solutions, by meeting the three requirements in a single structure: lightweight, load carrying and shape adaptable.

This section considers the materials that allow large deformations for morphing wind turbine blades. As previously discussed, the ideal material for a morphing structure must meet three conflicting requirements: load-carrying capability, deformability and low weight. It is reported by Thill *et al.*<sup>18</sup> that elastomeric and anisotropic materials have potential for morphing on aircraft wings, and these are also considered here. The concepts detailed in the following focus on those materials where primary loads are transmitted in the span-wise direction, whereas a morphing function is achieved via chord-wise flexibility.

#### 3.1. Elastomeric materials

Elastomers are a class of polymer with a low density of cross links; hence, they have the ability to undergo large strains without deforming plastically. The low stiffness of elastomers (0.5 to 50 MPa) makes them easily deformable (up to 1000% elongation), and so they are good candidates for morphing skins where the actuation forces should be as low as possible. However, this also means elastomers alone are not suitable for carrying aerodynamic loads. Kikuta<sup>23</sup> experimentally tested

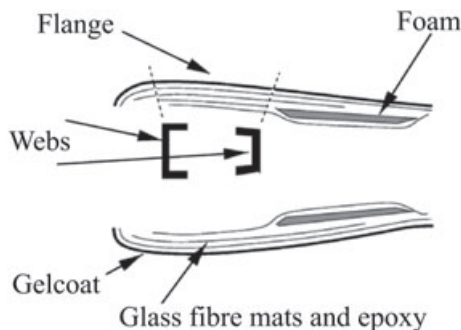


Figure 2. Typical current wind turbine blade composition.<sup>1</sup>

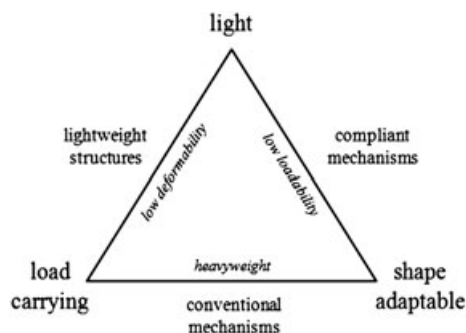
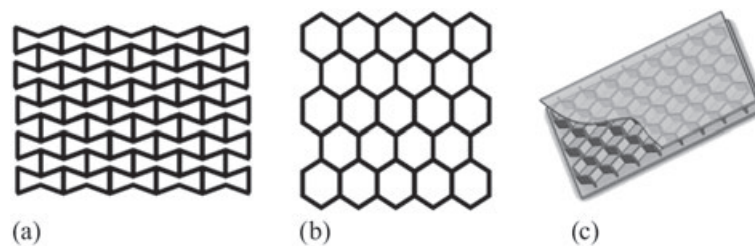


Figure 3. Shape adaptation diagram.<sup>22</sup>

several thermoplastic polyurethanes, copolyesters and woven materials commercially available. The characteristics of each material were investigated, and their viability as morphing skins for aircraft was analysed. The author first defined the properties that a morphing skin should possess:

- High out-of-plane stiffness to withstand aerodynamic loads and low in-plane stiffness to reduce actuation forces.
- Toughness and resistance to abrasion and to chemicals.
- Resistance to different weather conditions.
- High strain capability and recovery rate.
- Fatigue resistance.

By testing each material, a comparison was made, and the author concluded that none of the selected materials fulfilled all of the previously mentioned requirements. In Kikuta's report, the Tecoflex<sup>®</sup> 80A was found to be the best compromise in terms of strain capability, recovery rate and material type. The author suggested combining the Tecoflex 80A with a woven material like Spandura<sup>®</sup> to achieve a high strain capability and recovery rate from the polymer with the high strength from the fibres. This was achieved by Peel and Jensen<sup>24</sup> and Peel *et al.*<sup>25</sup> In these studies, they successfully manufactured silicone and urethane glass reinforced composite to a thickness of 0.8 mm using filament winding and autoclave techniques. The in-plane Young's modulus of the unidirectional (UD) glass–silicone composite was 1.94 MPa transverse to the fibre direction and 1830 MPa in the fibre direction. The Young's modulus for the UD glass–urethane was 2.25 and 3400 MPa transverse to the fibre direction and in the fibre direction, respectively. Flexural properties are not given, but the low flexural stiffness of the material could be a limiting factor if used for a skin application: the low flexural stiffness could lead to buckling and deformation of the skin when aerodynamic loads are applied. Highly anisotropic materials are also recommended for morphing skins by Ghandi and Anusonti-Inthra<sup>26</sup> and Murray *et al.*<sup>27</sup> Their work is detailed in Section 3.2.2.



**Figure 4.** (a) Zero Poisson's ratio honeycomb. (b) Classic honeycomb structure. (c) Flexible skin concept presented by Olympio and Gandhi.<sup>29</sup>

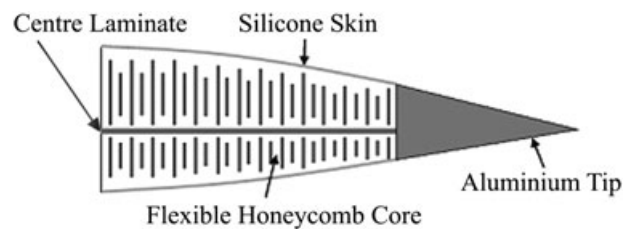


**Figure 5.** Flexible trailing edge concept—silicone skin with honeycomb core on a centre laminate.<sup>31</sup>

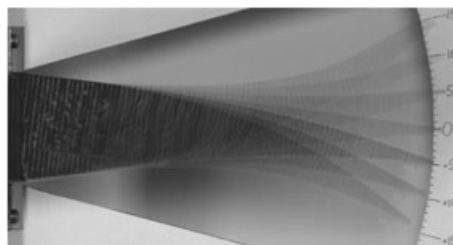


**Figure 6.** Wind turbine flexible flap made of honeycomb core covered by a carbon fibre reinforced polymer skin on the suction side and silicone on the pressure side.<sup>32</sup>

### 3.2. Anisotropic materials

The ideal morphing structure would require minimal actuation force in the morphing direction but remain stiff in other directions to withstand external loads. This is where anisotropic structures and materials can be used. As opposed to isotropic materials, the stiffness of anisotropic materials is direction dependent. Thus, by designing structures with low stiffness where deformation is required but high stiffness in the direction where loads need to be reacted against, the structural properties are tailored and actuation forces minimised. Structures using anisotropic cores and skins have been proposed in several research studies and are detailed next.

#### 3.2.1. Anisotropic cores.

Honeycomb structures present characteristics making them potential contenders for morphing concepts. An interesting example of such structures was suggested by Olympio and Gandhi.<sup>28</sup> They presented analytical and finite element models of 'hybrid' and 'accordion' cellular honeycomb cores. By tailoring the geometry of the honeycomb cells, they achieved an overall zero Poisson's ratio structure; hence, an ideal candidate for a morphing skin where the formation of transverse curvature is often undesirable. They concluded that their 'accordion' type of honeycomb, shown Figure 4(a), is more suitable for a morphing application as it presented a better out-of-plane stiffness in the non-morphing direction than conventional (Figure 4(b)) or hybrid structures. Another detailed analysis of flexible skins using honeycomb cores was presented in Olympio and Gandhi,<sup>29</sup> and the concept is illustrated in Figure 4(c). In this paper, Olympio and Gandhi detailed the influence of honeycomb geometric parameters.

An example of commercially available honeycomb that could be used for morphing is the Hexcel Flex-Core®.<sup>30</sup> This cellular product can be deformed into small radii without deformation of the cell walls, loss of mechanical properties or significant anticlastic behaviour (i.e. formation of a double curvature under a one directional bending moment). Covered with a thin elastomeric skin, as suggested in Figure 4(c), a honeycomb core was used as part of a morphing trailing edge concept by Bartley-Cho *et al.*<sup>31</sup> The compliant structure was composed of a central laminate leaf spring, a flexible core, and was covered with a silicone skin, as illustrated Figure 5.

Daynes and Weaver<sup>32</sup> used an aramid hexagonal cell honeycomb core covered on one side by a 0.25 mm thick woven carbon fibre reinforced polymer (CFRP) skin and on the other side by a silicone skin. The prototype is shown in different positions in Figure 6. To eliminate the anticlastic behaviour of the honeycomb when the flap was actuated, the core has been sliced in the chord-wise direction into 20 mm wide sections. Although the CFRP skin provided enough stiffness to avoid buckling under aerodynamic loads, it was compliant enough to allow morphing at a low actuation cost. Finally, the silicone skin provided a seamless external profile while allowing for large in-plane strains.

#### 3.2.2. Anisotropic skins.

The properties of an ideal flexible skin for aerofoil camber morphing are described in Gandhi and Anusonti-Inthra<sup>26</sup> and Murray *et al.*<sup>27</sup> These ideal properties are highly anisotropic with low in-plane axial stiffness yet high out-of-plane flexural stiffness. A reduced axial stiffness allows morphing at low actuation cost; however, a lower limit on the skin's in-plane axial stiffness may be required to prevent unacceptable global camber deformation under aerodynamic loads. It was also highlighted that a high flexural stiffness is recommended to prevent the skin from locally deforming due to aerodynamic pressure loads, especially in unsupported sections. It also avoids buckling of the skin as the aerofoil cambers under actuation force.

A concept of extremely anisotropic skin was presented by Yokozeki *et al.*<sup>33</sup> The stiffness of their skin concept was tailored by using a corrugated composite sheet. The stiffness in the direction of the corrugation was further increased with stiff composite carbon rods, as shown in Figure 7. Aerodynamic characteristics of the surface were improved by filling one side of the structure with a low stiffness rubber to achieve a smooth surface without increasing bending stiffness in

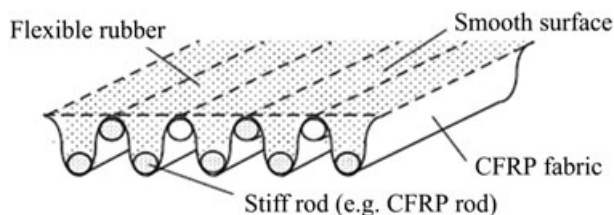


**Figure 7.** Reinforced corrugated structure with one side rubber filled for aerodynamic properties enhancement.<sup>33</sup> CFRP, carbon fibre reinforced polymer.

the direction of morphing. Experimental and analytical results confirmed the highly anisotropic behaviour of corrugated structures.

Thill *et al.*<sup>34,35</sup> also carried out experimental, analytical and numerical investigations on corrugated composite sheets. They concluded that the large deformations achieved with their aramid/epoxy corrugated laminate were due to the opening of the corners of the trapezoidal pattern used for the corrugations, a consequence of delamination and compressive failure of the fibres in these regions. However, it was emphasised that this phenomenon might not occur with glass or carbon fibre laminates. A solution proposed to avoid fibre failure was to tailor the stiffness of the corners by using a more compliant matrix material.

Recently, Ge *et al.*<sup>36</sup> modelled and tested a corrugated composite made of glass fibre fabric. A finite element model was created using ANSYS software, and correlation between computational results and experiment was found. It was concluded that corrugated composites can withstand the elongation necessary to bend a trailing edge up to  $10^\circ$  without failure or permanent deformation. Linear relationships between the number of corrugations, the thickness of the composite and its elongation were found. Compared with a flat composite laminate of the same characteristics (material, number of plies, manufacture and test procedure), the elongation of the corrugated laminate was found to be 600 times larger.

In Murray *et al.*,<sup>27</sup> a novel flexible matrix composite (FMC) was analysed. The fibres of the FMC were pre-stressed in tension in the non-morphing direction. This had the advantage of reducing the out-of-plane deformations when loading was applied while not increasing the actuation force in the morphing direction. An analysis was developed and validated against experiments; a parametric study utilising that analysis compared the influence of several parameters such as pre-tension, load, matrix modulus and fibre modulus.

Anisotropic skins seem ideal for morphing applications. However, the need for a supporting structure to avoid the local deformations induced by the aerodynamic loads could be a limiting factor and could lead to heavy and complex design. This is also the case when using the FMC described in Murray *et al.*,<sup>27</sup> where the structure needs to withstand both the exterior loads and the pre-stress loads.

### 3.3. Multistable materials

Multistable structures and materials are capable of holding several stable positions. In their current form, multistable materials exhibit large deformations but only need low actuation forces. This can reduce the number of applications since the loads applied to the structure can be greater than the forces needed to snap the structure between stable configurations. However, applications exist; examples from Daynes *et al.*,<sup>37</sup> Schultz,<sup>38</sup> and Guest and Pellegrino<sup>39</sup> are reported below. Multistability is achieved by designing a structure that has multiple strain energy minima. This can occur in composites as a result of a combination of residual stresses induced during the cure cycle and geometric non-linearity in a non-symmetric FRP lay-up, as detailed by Dano and Hyer,<sup>40</sup> as a result of Gaussian curvature effects, as detailed by Seffen<sup>41</sup>, as a result of fibre pre-stress, as explained by Daynes *et al.*<sup>42</sup> or as a result of plastic deformation, as reported by Guest and Pellegrino.<sup>39</sup> Several numerical and experimental studies have analysed the bistability of multilayered composites plates with unsymmetric stacking sequences, and detailed explanations of bistable and multistable composites can be found in Daynes *et al.*,<sup>37</sup> Schultz,<sup>38</sup> Dano and Hyer,<sup>40</sup> Diaconu *et al.*,<sup>43</sup> Mattioni *et al.*,<sup>44</sup> Potter *et al.*<sup>45</sup> and Potter and Weaver.<sup>46</sup>

An application of bistability was investigated by Schultz.<sup>38</sup> His device was constructed by assembling two rectangular, carpenter-tape-shaped shells with their concave surfaces facing towards each other, as illustrated in Figure 8. Each shell was made of a  $0/90^\circ$  graphite/epoxy FRP lay-up, developing bistability at room temperature. As the short edges of the shells were pressed together, twist developed along the structure. By applying an opposite twisting moment at the short edges, the structure snapped from one stable twisted configuration to the other. Actuation was realised using piezoceramic macro fibre composite patches bonded on the inside of each shell, across the diagonal. The device could twist  $\pm 5^\circ$  at a



Figure 8. Bistable twisting structures presented by Schultz.<sup>38</sup>

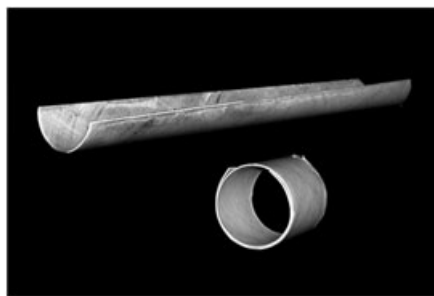


**Figure 9.** Extended and coiled configuration of a bistable composite shell.<sup>49</sup>

maximum frequency of 10 Hz. The influence on the twisting moment, the twist angle of the tip of the plate and the thickness of the structure were analysed. An analysis was also performed using ABAQUS/Explicit<sup>47</sup> finite element software, and correlation with the experiments was found. Scaling up this concept for an application on a wind turbine has yet to be investigated; however, one can easily imagine a blade tip device using this structure to mitigate aerodynamic loads.

Daynes *et al.* achieved bistability by pre-stressing part of the fibres in a laminate made of prepreg material before the curing process.<sup>42</sup> The long edges of a rectangular plate were subjected to a constant strain before and during cure at elevated temperature. Once cooled to room temperature, the strains were released, inducing a varying state of stress across the width of the plate; thus, bistability occurred. This novel type of composite has the advantage of being insensitive to hygrothermal variability and exhibits a much higher snap-through load than laminates with a  $[0_n/90_n]$  lay-up, which rely only on the difference in coefficient of thermal expansion (CTE) between the matrix and the fibres to develop bistability. This concept was used on a helicopter blade flap<sup>37</sup> and is detailed in Section 4.2.2 of this article.

Potter and Weaver investigated the influence of discrete UD strips embedded in  $0/90^\circ$  laminates.<sup>46</sup> They noticed that considerable distortions could be achieved, even when the strips were placed in the neutral axis of the laminate. These distortions existed in at least two states with a snap-through phenomenon between them. In principle, an unlimited number of stable states could be achieved when dividing the laminate into ‘cells’ of distortion by locally embedding small strips of UD material. The authors also investigated the variations of internal stresses in the laminate caused by the difference in CTE between the tool (usually aluminium) and the laminate itself. As the laminate is heated at high temperature for curing, the difference in CTE results in the tool expanding more than the laminate. As a consequence, strains arise in the laminate while curing, inducing a varying state of stress at room temperature; thus, multistability is possible.

The behaviour of multistable shells actuated by embedded piezoelectric actuators under a temperature differential was studied by Varelis and Saravanos.<sup>48</sup> The analytical tool that they developed accurately modelled the highly non-linear relationship between the shape changes of the shell, the electric potential applied to the actuator and the thermal loads.

Other applications of bistable structures were investigated by Guest and Pellegrino<sup>39</sup> and Iqbal and Pellegrino,<sup>49</sup> focussing on the behaviour of thin cylindrical shells, as shown Figure 9. They developed an analytical model to predict the stable configurations of tape springs made of anti-symmetric laminates. As per standard steel tape measures, these structures exhibited a straight, stable configuration; however, by tailoring the lay-up used to manufacture the shells, a second, coiled configuration also existed. This remarkable property has applications in the field of deployable booms, as explained in detail in Iqbal and Pellegrino.<sup>49</sup>

In Guest *et al.*,<sup>50</sup> a metallic structure with zero stiffness in one degree of freedom was investigated. Because of a particular combination of geometry and initial pre-stress, the shell manufactured could hold any position between a coiled state and an extended straight state, as shown in Figure 10. An analytical model was described and validated experimentally. The zero stiffness structure was achieved by keeping the stored strain energy at a constant level with respect to the morphing direction, i.e. pre-stressing the shell and adding a defined amount of curvature to it effectively created a zero torsional stiffness throughout the shape change. In this special case, bistability was not effected, but the structure was left without any torsional stiffness.

In their present state, few concepts using multistable composites have reached the prototype stage. However, their intrinsic structural properties and their ability to snap between positions with little delay make multistable structures potential candidates for wind turbine morphing applications.

#### 4. REVIEW OF AERODYNAMIC CONTROL CONCEPTS

Current wind turbines are highly reliable: Hahn *et al.*<sup>51</sup> reported a technical availability reaching 98%, meaning a yearly downtime of only 1 week for maintenance and repair. Therefore, the increase in cost, weight or maintenance required by

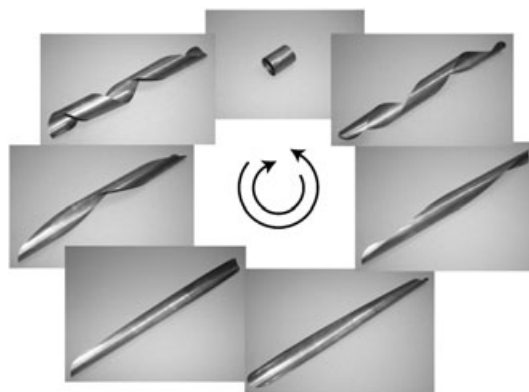


**Figure 10.** Fine metallic cylindrical shell presenting zero stiffness along the axis of twist. The shell is held in place by no more than the friction with the underlying surface.<sup>50</sup>

a load alleviation device should be justified by a significant load reduction capability. Other parameters must be considered in the design of aerodynamic control devices for wind turbines including simplicity, aerodynamic efficiency and the required bandwidth of the control system.<sup>21</sup> Moreover, moving parts and the danger of lightning strikes should be reduced or avoided as much as possible. For these reasons, morphing structures present suitable properties, offering reduced complexity and lower weight compared with mechanisms and better efficiency due to a continuous aerodynamic profile. The design of morphing structures, on its own, faces clear challenges in delivering the required shape changes while maintaining strength, stiffness and low weight. Compared with discrete mechanisms where high-stiffness members are articulated around elements of finite degrees of freedom, morphing structures must meet contradictory requirements: be compliant to reduce actuation forces and achieve shape change, but be sufficiently stiff to carry loads and maintain structural integrity. Morphing structures must also be lightweight and reliable to compete against conventional mechanisms.

The morphing of aerofoils can be classified into two main groups:

- *In-plane morphing*: including span-wise change, chord-wise change and sweep, as illustrated in Figure 11(a)–(c), respectively.
- *Out-of-plane morphing*: including span-wise change, chord-wise change and twist, as shown in Figure 11(d)–(f), respectively.

## 4.1. In-plane transformation

### 4.1.1. Span-wise change.

Telescopic structures have been proposed to enable significant changes in wing or blade length. The aerofoil consists of several segments of reducing cross section, each sliding inside the adjacent inner segment with a minimum clearance. Neal *et al.*<sup>52</sup> designed and tested an adaptive aircraft able to increase its wing span by 38%, using a pneumatic cylinder for actuation. Wind tunnel results showed that low drag can be maintained for a range of lift coefficients.

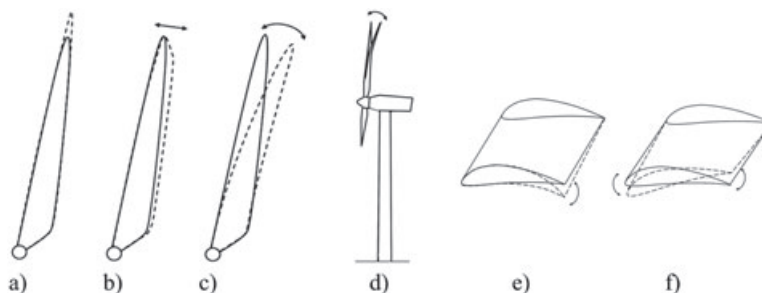


**Figure 11.** The different shape changes considered. In-plane morphing: (a) span-wise, (b) chord-wise and (c) sweep. Out-of-plane morphing: (d) span-wise, (e) chord-wise and (f) twist.



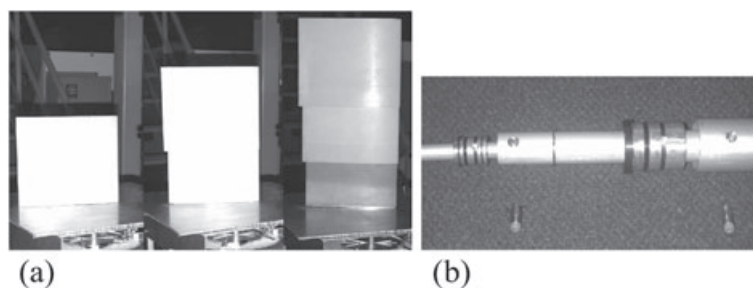


**Figure 12.** (a) Telescopic wing and (b) details of the linear bearings used by Blondeau for the telescopic spar.<sup>53</sup>

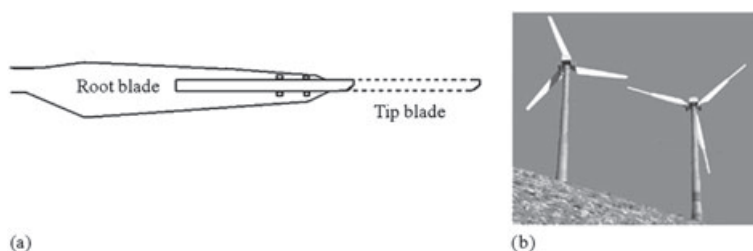


**Figure 13.** (a) Variable diameter rotor concept. (b) Fully extended prototype next to a standard wind turbine.<sup>54</sup>

Using the same principle for a telescopic wing, Blondeau *et al.*<sup>53</sup> developed a wing for an unmanned air vehicle (UAV). The structure, shown in Figure 12(a), is extended by 114% while supporting aerodynamic loads. The deployment and retraction of the wing were performed by two inflatable spars, which also acted as structural components, thereby reducing weight. The telescopic spar design consisted of three concentric circular aluminium tubes of decreasing diameter deployed under pressure. For misalignment to be avoided, ceramic bearings were inserted between each pair of tubes, as shown Figure 12(b). Tight tolerances between the wings were achieved by moulding the wing's skin between a male and female aluminium moulds. Experiments showed a 25% decrease in the lift-to-drag ratio of the fully extended wing against its rigid counterpart. Blondeau explained this effect by the additional drag created at the seams of the wing sections.

Because of its high load reduction potential, span-wise morphing was investigated in a collaborative project between Energy Limited, DOE and Knight and Carver, as reported by Johnson *et al.*<sup>54</sup> The prototype operated by extending/retracting a tip blade out of a root blade, as shown in Figure 13(a). During low wind speeds, a large rotor diameter provided more capture area, which resulted in larger aerodynamic loads and an increase in energy capture. However, this operation generated larger blade root and tower base bending loads. At higher wind speeds, the rotor diameter was decreased to avoid excessive loads. An 18 m diameter prototype was field tested and was able to increase the blade length from 8 to 12 m. Results showed a power production increase of 20% to 50% at low wind speeds ( $7\text{--}9\text{ m s}^{-1}$ ) compared with standard blades, even though a decrease in performance was noticed at rated wind speed, mainly because of the poor aerodynamic performance of the prototype. For this concept to be scaled up to megawatt-sized wind turbines, several engineering challenges remain, including implementing complex control strategies, the need to maintain a high aerodynamic efficiency, limiting the increase in blade weight, and general issues with durability and reliability of the system as a whole. This morphing concept has the advantage of offering great load reduction potential using known technologies but would not be appropriate at reducing high-frequency phenomena due to the retraction time of the blade tip.

Bubert's concept<sup>55</sup> consisted of an aerofoil-shaped honeycomb structure reinforced by carbon fibre rods in the span-wise direction, as shown in Figure 14(a),(b). A smooth surface for aerodynamic efficiency was achieved by covering the profile with a low in-plane stiffness elastomeric skin. Although the components were analytically studied and modelled and a skin section demonstrator was manufactured, a prototype of the aerofoil section has yet to be produced and tested in a wind tunnel to confirm the skin characteristics and the mechanism output capabilities. The clear advantage of this concept is the smooth distribution of deformations induced by the shape change over the span of the morphing structure, whereas the design implemented for the variable span wind turbine rotor used two rigid parts, thus presenting a discontinuity of the aerodynamic profile.

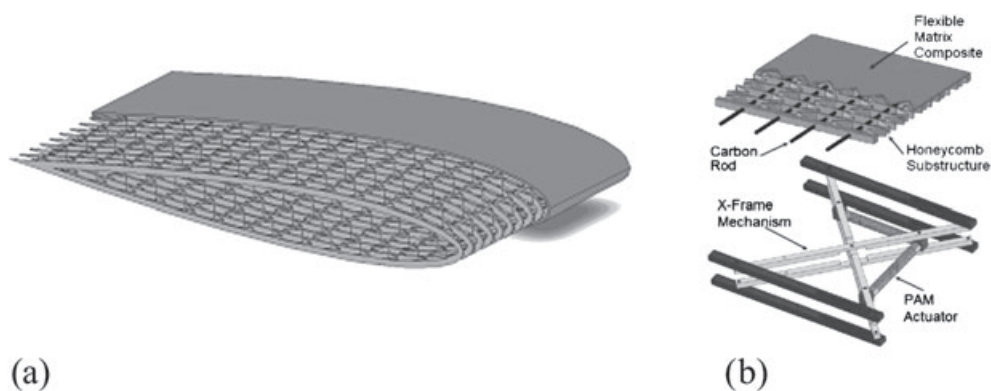


**Figure 14.** (a) Span-wise morphing achieved with a honeycomb structure covered with an elastomeric skin. (b) Prototype used for the test of the honeycomb structure and actuator.<sup>55</sup> PAM, pneumatic artificial muscle.

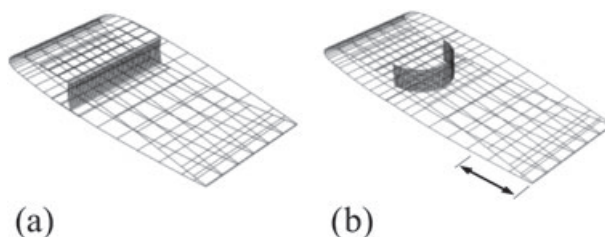


**Figure 15.** Model of an aerofoil section using a bistable plate for chord-wise morphing in (a) the retracted and (b) extended configurations.<sup>43</sup>

#### 4.1.2. Chord-wise change.

Chord-wise area increase may be obtained in conventional aircraft by means of leading and trailing edge flaps actuated by complex and heavy lead-screw systems. Moreover, the discontinuities introduced in the aerodynamic profile by these devices generate noise and loss of efficiency compared with a seamless, morphing wing. Little research has been carried out in this field to achieve chord-wise change without using mechanical flaps. In Diaconu *et al.*,<sup>43</sup> bistable composite materials were used as a mean of chord-wise morphing an aerofoil. The length change of the chord was realised by inserting a rectangular bistable plate into the airfoil section, in a vertical position along the main spar, as shown in Figure 15. The airfoil was composed of two separate parts: a fixed leading part, including the main spar and a morphing trailing edge part, attached to the centre of the bistable plate. Snapping the bistable plate from one equilibrium state to the other resulted in a chord-wise displacement of the centre of the plate, thus extending or retracting the trailing part of the aerofoil. During actuation between the two stable states, the corners of the bistable plate were allowed to slide horizontally along the spar, and the top and bottom surfaces of the trailing part could slide chord-wise inside the leading part of the airfoil. Although this study did not lead to the manufacture and test of a prototype, it benefited from reduced actuation cost, stability of the configurations and short deployment/retraction time; thus, it is a potential concept for a wind turbine application.

Shape memory foams and shape memory polymers (SMP), which can be 'programmed' to have different shapes, were tested by the researchers of the Cornerstone research group for chord-wise morphing.<sup>56–58</sup> By heating the SMP above its transition temperature (which can be a glass transition or a melting temperature), it becomes soft and can be deformed by the application of a load. When the polymer is cooled into its new shape and the load is removed, the polymer will remain in this new temporary shape. This concludes the 'programming' process. If the polymer is heated back above the transition temperature, the polymer will return to its permanent or memorised shape. This is called the recovery process. An initial concept from Cornerstone, shown in Figure 16(a), consisted of a shape memory foam core covered with a SMP skin to obtain a smooth surface. Although the foam extended upon heating, it could not return to its original shape, demonstrating the limitations of the shape memory foam, as reported by Perkins *et al.*<sup>56</sup> A second concept was investigated, in which a set of sliding aluminium ribs (Figure 16(b)) were used instead of shape memory foam. The aerodynamic loads were transferred from the SMP skin to the underlying aluminium structure through a honeycomb core, allowing the chord-wise expansion. Actuation of the ribs was carried out using miniature motors driving lead screws, whereas actuation of the skin was still

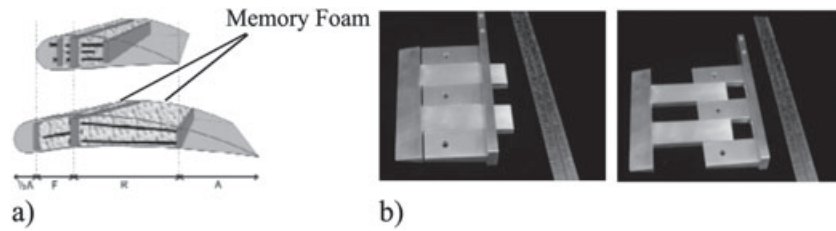


**Figure 16.** (a) Initial concept developed by Cornerstone using a memory foam core. (b) Second concept using sliding ribs.<sup>56</sup>

under investigation. Embedded heating wires were studied; however, for weight to be saved and for a better heat distribution to be achieved, a self-heating skin, using the thermal and electrical conductivity of the SMP, was also investigated.

#### 4.1.3. Sweep.

This morphing technology has been thoroughly investigated for conventional aircraft and UAVs; however, only discrete mechanisms have been used for production aircraft, such as the Tornado, F14 or B1. The prototype UAV manufactured by Neal *et al.*<sup>52</sup> used a similar design to that. The rigid wings were able to rotate by  $40^\circ$  of sweep around a pivot point. The shape change was achieved with a three-bar linkage, shown in Figure 17, where one of the links was a lead-screw actuator.

A more innovative and integrated concept was proposed by NextGen Aeronautics and detailed by Flanagan *et al.*<sup>59</sup> Their UAV could undergo sweep angle change ( $15^\circ$  to  $35^\circ$ , as shown in Figure 18) during flight in less than 15 s. The 2.8 m span morphing wing was made of an endoskeleton wing box stiffened by means of ribbons and covered with an elastomeric skin. Full sweep induced a 40% change in wing area. Morphing was achieved with a single electric motor, with both wings undergoing essentially identical configuration changes. Successful in-flight sweep morphing confirmed the capacity of the elastomeric skin to withstand aerodynamic loads while undergoing a large area change.

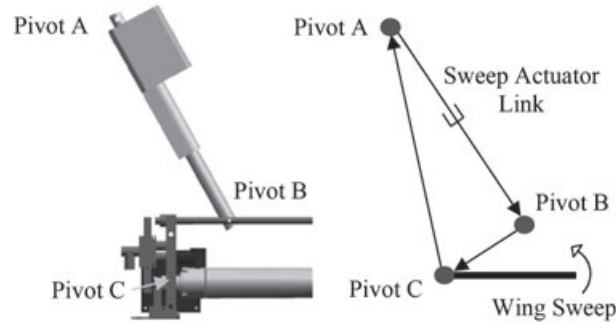


**Figure 17.** Schematic views of the three-bar linkage mechanism allowing sweep change around pivot C.<sup>52</sup>

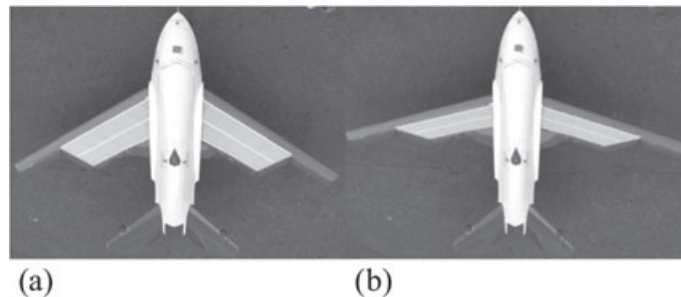


**Figure 18.** NextGen Aeronautics MFX-1 prototype showing the two extreme sweep angles: (a)  $45^\circ$  and (b)  $15^\circ$ .<sup>59</sup>

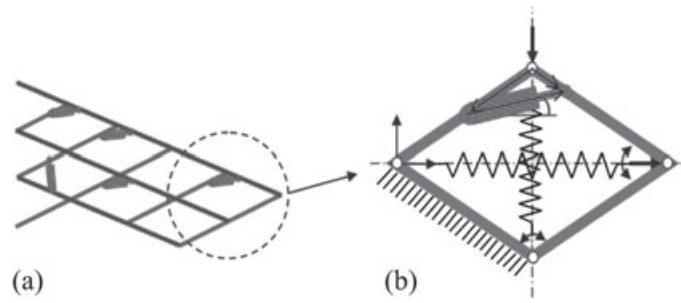


**Figure 19.** (a) Wing scissor mechanism for in-plane span-wise morphing. (b) Unit cell showing the actuation principle.<sup>60</sup>

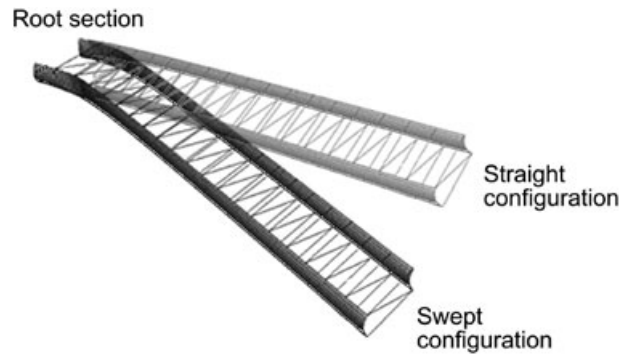


**Figure 20.** Morphing wing box using bistable composite spars.<sup>61</sup>

A scissor-like mechanism was investigated by Joo and Sanders<sup>60</sup> to alter the wing shape in an analytical model. They studied the optimal location of a distributed network of actuators within the morphing wing scissor mechanism, shown in Figure 19(a). Skin stiffness was modelled as springs exerting reaction forces in different directions on the unit cells, as illustrated in Figure 19(b), and aerodynamic loads were added to the system as concentrated forces. By taking into account actuator stroke and blocking force, an algorithm was written to optimise the location of the actuators within the network of cells. However, the structure's morphing skin was not addressed in this study.

The aforementioned examples describe sweep angle morphing achieved by means of pivots and complex set of linkages; therefore, there is an associated weight penalty and added system complexity with this approach. An alternative design was adopted by Mattioni *et al.*<sup>61</sup> Their wing box concept consisted of two beams having a curved cross section and linked with a truss-rib structure, as shown in Figure 20. The application of a predefined bending moment to the structure, due to increased drag from enhanced speed or via an actuator, locally deformed the cross section of the spars, enabling a flexural hinge at the root section to appear. Hence, the wing box could be held straight or swept without the need for discrete hinges.

Although sweep morphing proved to enhance aircraft performance, wind turbine blades might not benefit from this morphing concept, as the time delay to morph from the straight to the swept configuration may be too long to respond to sudden changes in wind conditions.

## 4.2. Out-of-plane transformation

### 4.2.1. Span-wise change.

Span-wise bending has been mainly studied for aircraft applications. National Aeronautics and Space Administration researchers demonstrated that a hyperelliptically swept planform wing with a cambered span and a separate hyperelliptical span-wise profile, shown in Figure 21(a),(b), has aerodynamic advantages over a flat wing, according to Lazos.<sup>62</sup> Such a wing, called hyperelliptical cambered span (HECS), inspired researchers to investigate the span-wise morphing of wings. In Wiggins *et al.*,<sup>63</sup> a scissor-like mechanism was used to morph a wing to a HECS shape. The mechanism, illustrated in a straight configuration in Figure 21(c), was designed such that only one input, in the form of an actuator displacement, was required into the first linkage for the rest of the structure to deform to the desired shape. However, the study did not consider how the morphing structure would be covered to obtain a compliant aerofoil profile.

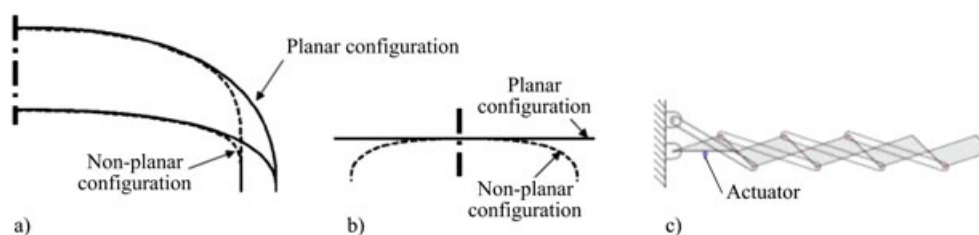


**Figure 21.** (a) Top view and (b) front view of the hyperelliptical cambered span wing. (c) Illustration of the principle behind the model developed by Wiggins.<sup>63</sup>

In Sofla *et al.*,<sup>64</sup> the span-wise bending of a UAV wing using shape memory alloy (SMA) as an actuator has been investigated. An underlying structure made of lightweight truss beams could adopt several configurations, including the HECS. Their aim was to verify the predicted aerodynamic performances of the HECS against wind tunnel test of a morphing prototype and was reported to be the next stage of this project.

To the knowledge of the authors, this type of morphing solution has not been applied to wind turbine blades, and the benefits of it are yet to be demonstrated. As per the sweep morphing, response to sudden changes in wind conditions would be too slow to be efficient in a feedback control system; thus, the added complexity of such structures would be hard to justify.

#### 4.2.2. Chord-wise change.

Initial investigations of chord-wise change in wind turbine blades were inspired by aircraft experience, using small moveable surfaces to control lift. Early investigations on flaps applied to wind turbines were performed by the National Renewable Energy Laboratory during the 1990s.<sup>65,66</sup> At the time, these devices were analysed for power regulation and aerodynamic braking. Several wind tunnel experiments and field tests were performed to quantify the performance of the devices. Although no active control was performed (the ailerons were in fixed positions), these experiments are of importance because they initiated investigations on the aerodynamic parameters associated with flaps and their influence on wind turbine performance.

Two designs are investigated in this area: discrete flaps (ailerons) and morphing trailing edges. Discrete hinged flaps require a bending moment acting around a pivot point to achieve the desired position and therefore are subjected to wear and corrosion, high maintenance and a compromised lift-to-drag ratio due to the sharp change in the camber. On the contrary, a continuous deformable trailing edge offers a smooth change in camber, potentially improving the lift-to-drag ratio of the aerofoil.

By increasing or decreasing the effective camber of the aerofoil, trailing edge flaps can achieve changes in blade lift with flap deflections of only a few degrees. Compared with the classic full span pitch control that adjust the pitch angle of the blade via a mechanism at the blade root, ‘morphing’ flaps require less power, have intrinsically better structural features and offer a much faster response time. Moreover, flaps can be sectioned over the blade span and individually controlled to respond to local aerodynamic fluctuations, enhancing the overall performance of the blade. This is why morphing trailing edges are considered strong potential concepts for blade load reduction by wind turbine laboratories such as Risø DTU, The Delft University Wind Energy Research Institute and Sandia National Laboratories.

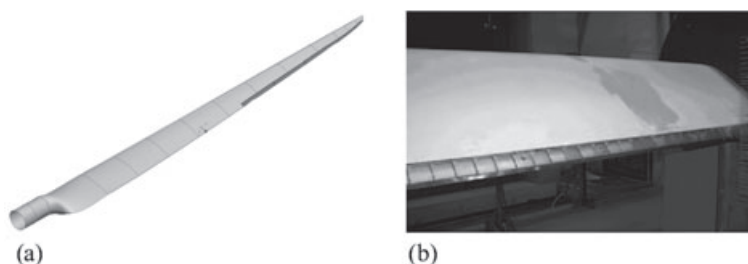


**Figure 22.** (a) Vestas V66 modelled for the ADAPWIND project. Twelve meters of the blade tip was equipped with independently controlled flaps (shown in dark grey).<sup>2</sup> (b) Risø B1-18 blade equipped with active trailing edge flaps.<sup>7</sup>

At Risø DTU, the 3D analysis of a Vestas V66 blade was completed, comparing the efficiency of different combinations of flap length and positions along the last 12 m of the blade, as shown in Figure 22(a). The study highlighted a potential 64% reduction of the span-wise root bending moment using an 11 m long flap located at the blade tip, as reported by Buhl *et al.*<sup>2</sup> Wind tunnel tests were also carried out on a Risø B1-18 blade equipped with deformable trailing edge tabs actuated by piezoelectric bender patches (Figure 22(b)). For the experiment, 36 piezoelectric actuators were required to obtain the 1.9 m span flap. Steady state tests showed the flap could deflect  $+1.5^\circ$  to  $-2.5^\circ$  at a Reynolds number of  $1.66 \times 10^4$ . This corresponded to a change in lift coefficient of  $+0.036$  and  $-0.066$ , respectively. The trailing edge flap covered 9% of the aerofoil chord but was capable of reducing blade loads by up to 80% when the actuator control was used appropriately, as demonstrated by Bak *et al.*<sup>7</sup>

The Delft University Wind Energy Research Institute has also studied the application of morphing flaps to wind turbine blades. Several articles can be found in the literature, including the ones from Barlas and van Kuik,<sup>67</sup> Barlas *et al.*<sup>68</sup> and van Wingerden *et al.*<sup>69</sup> A non-rotating dynamically scaled wind tunnel model was manufactured; actuation was provided by four piezoelectric benders (Thunder<sup>®</sup>), and a smooth aerodynamic surface was achieved with a foam and latex skin covering the actuators, as detailed in Figure 23. The wind tunnel test demonstrated that vibrations due to randomly varying aerodynamic loads could be reduced using a closed-loop control system and showed that the bending strains at the blade root could be reduced by up to 95%.

As part of the European UpWind project,<sup>70</sup> a wind turbine blade section with a morphing flap was modelled, manufactured and tested, as reported by Hulskamp.<sup>17</sup> The actuation relied on SMA wires embedded into the trailing edge skin; therefore, the blade structure remained unchanged, as illustrated in Figure 24. Mechanical sleeves and adhesive bonding joints were used in the manufacture of the SMA composite to transfer the load from the wire to the laminate. This allowed the use of bigger wires, as the forces generated by the wires were evenly distributed and therefore achieved a higher flap deflection. The final blade prototype had a 1 m span, and wind tunnel tests demonstrated the increase in lift achievable. With an air flow of  $30 \text{ m s}^{-1}$ , the activation of the wires enhanced the lift by  $\sim 15\%$  at  $5^\circ$  angle of attack. The downside of conventional SMA composites is the poor heat conductivity of the material; therefore, the time to cool down the wires between activations limits the operational frequency of such a structure.

In an effort to achieve a better operational frequency using SMA composites, R-phase SMA composites were used by the researchers at VTT Technical Research Centre of Finland.<sup>71</sup> A remarkable property of this type of SMA is its faster heating and cooling characteristic, meaning a higher operational frequency and lower power consumption. A blade section with a morphing flap was modelled with ABAQUS<sup>47</sup> finite element software and manufactured. Wind tunnel tests resulted in deflections smaller than predicted, due to damage endured by the wires during preliminary testing. The maximum operational frequency achieved with the R-phase SMA actuated blade flap was close to 1 Hz, mainly limited by the

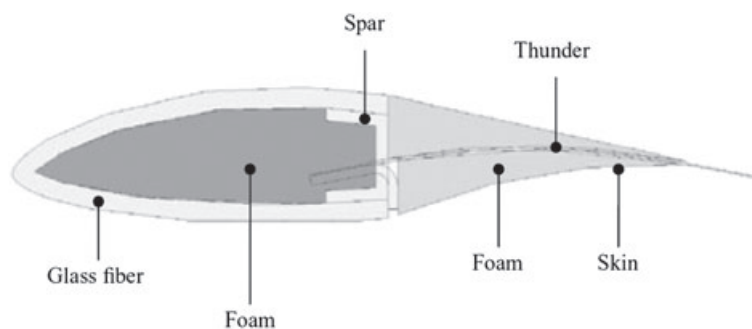


**Figure 23.** Cross-sectional view of the wind tunnel model used by Delft University Wind Energy Research Institute.<sup>69</sup>

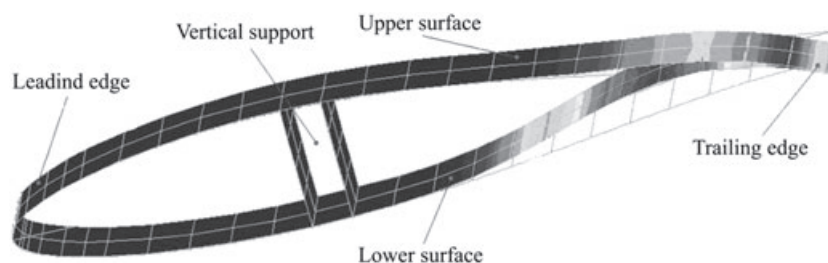


**Figure 24.** UpWind model of a blade section with shape memory alloy wires as actuators embedded into the trailing edge lower side.<sup>17</sup>

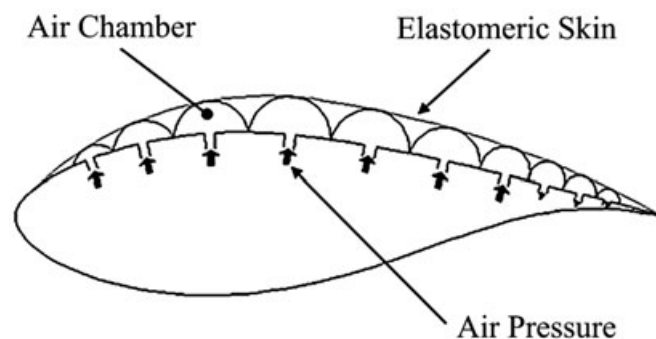


Figure 25. Inflatable camber control concept.<sup>72</sup>

heat dissipation capability of the laminate encapsulating the wires. The report concluded that R-phase SMA wires were a promising actuation concept for wind turbine actuation. However, the frequency of activation still limited the range of applications.

Another concept for camber control on wind turbine blades, by Marrant and Van Holten,<sup>72</sup> used inflatable bladders to morph the aerofoil shape. Inflatable structures have been investigated for UAV and space applications for their capacity to be stiff once inflated whilst occupying a small volume when deflated; one example given is by Cadogan *et al.*<sup>73</sup> In the present example, shown in Figure 25, several separate air chambers located on the upper or lower side of the aerofoil are inflated, pushing an elastomeric skin outward, hence changing the camber of the aerofoil. The stiffness of the flexible outer skin would be provided by the air chambers. The changes in lift coefficient as well as the maximum actuation frequency were estimated to be similar to conventional trailing edge flaps.<sup>71</sup> A clear advantage would be the smoother surface skin that would reduce the acoustic problems encountered with hinged trailing edge flaps. However, actuation would require an air pressure vessel held under pressure with an air pump. This might involve a complex system, and leakage could be a significant issue. Instead of air, higher density fluids could be used to ensure maximum rigidity, but this could result in a weight penalty.

For the weight, complexity and wear issues associated with discrete mechanisms of the type presented by Monner *et al.*<sup>74</sup> and Poonsong<sup>75</sup> to be solved, continuous deformable aerofoils using compliant structures have been extensively investigated by Kota<sup>76</sup> and Kota *et al.*<sup>77</sup> A compliant structure is a class of mechanism that relies only on elastic deformation of its constituent elements to transmit motion and/or force. These monolithic structures are, in fact, mechanisms without any joints—neither conventional nor flexural hinges. Using genetic algorithms to optimise the structure, Kota designed an aerofoil trailing edge capable of deflections in the range  $\pm 10^\circ$ , as illustrated in Figure 26. Wind tunnel results highlighted the benefits of this FlexSys variable geometry trailing edge flap; as the flap angle varied from  $-8^\circ$  to  $+8^\circ$ , the coefficient of lift increased from 0.1 to 1.1 without increasing the coefficient of drag. A conventional electromechanical actuator was used for the tests, reaching deflection speeds of  $20^\circ \text{ s}^{-1}$ . Adaptation to a wind turbine was studied in collaboration with Sandia National Laboratories and reported in Berg *et al.*<sup>78</sup>

Shili *et al.*<sup>79</sup> also analysed and designed a morphing trailing edge section, demonstrating the advantages of compliant structures and the effectiveness of the design method. With the utilization of MATLAB (MathWorks, Natick, Massachusetts, USA) and ANSYS (ANSYS, Inc., Canonsburg, Pennsylvania, USA) softwares, a design optimisation was engineered on the basis of a genetic algorithm. Material distribution was optimised to minimise the deviation from the

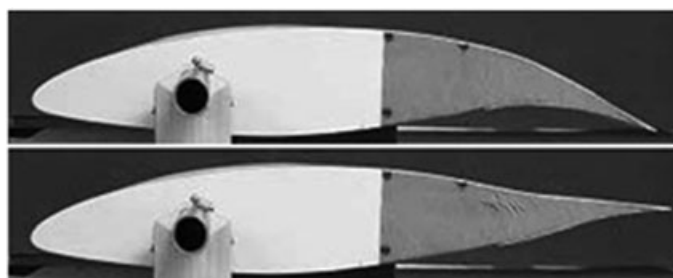


Figure 26. FlexSys variable geometry aerofoil.<sup>77</sup>

target shape under aerodynamic and actuator loads. An aerofoil section, shown in Figure 27, was manufactured, and close correlation between analytical and experimental results was found.

Gandhi *et al.*<sup>80</sup> designed a compliant trailing edge for a helicopter blade using a compliant scissor-like mechanism, shown in Figure 28(a),(b). A downward deflection of 3.65 mm on a 0.56 m chord length aerofoil section was achieved using a series of compliant units, each of them able to deflect by shortening or lengthening their member actuators (Figure 25(b)). Flexural hinges joined the active and passive elements while keeping the rotational degree of freedom necessary to obtain the shape change. Piezoelectric actuators were used to induce the bending of the trailing edge, and the structure could be actuated at a frequency reaching 50 Hz. An optimisation algorithm was performed on the passive elements of the units, seeking the optimal material distribution to maximise the deflection under actuation forces and minimise it under aerodynamic loads. The ANSYS analysis of the final structure predicted a 3.69 mm deflection, validating the algorithm against the experiment.

A successful design of compliant mechanism was engineered by Campanile and Sachau<sup>81</sup> and Campanile and Hanselka.<sup>82</sup> The belt-rib concept, shown in Figure 29, consisted of a 'camber-flexible' rib made of a closed shell (belt), reinforced by in-plane stiffeners (spokes). Because of the distribution of the spokes, out-of-plane deformations were allowed,

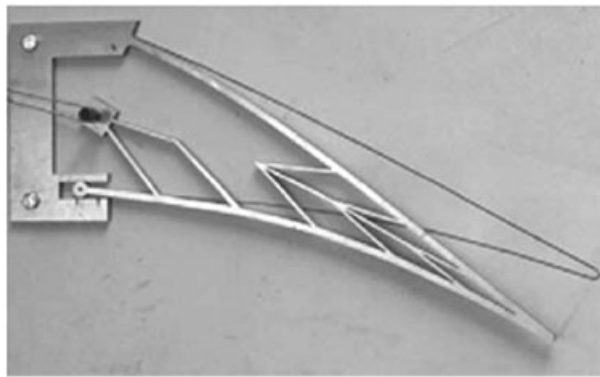


Figure 27. Compliant trailing edge section.<sup>79</sup>

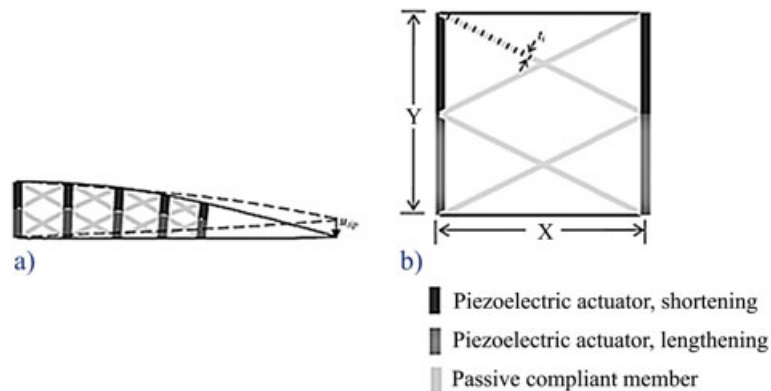


Figure 28. (a) Morphing trailing edge with compliant units mounted in series. (b) Undeformed compliant unit.<sup>80</sup>

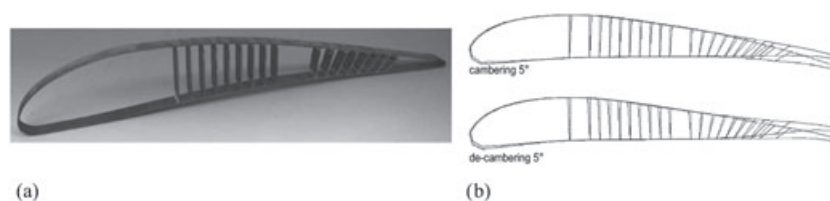
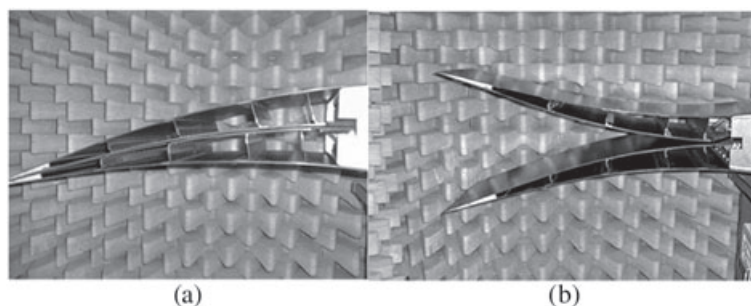


Figure 29. (a) Belt-rib prototype.<sup>81</sup> (b)  $\pm 5^\circ$  deflection of the trailing edge.





**Figure 30.** Morphing trailing edge concept for combine functions: (a) pitch, roll, yaw and (b) air braking.<sup>83</sup>

resulting in an overall camber change of the aerofoil section. For the rotational degrees of freedom to be enabled and for the trailing edge deflection to be achieved, the spokes were connected to the belt by means of flexural hinges; their position and orientation ensured no significant contribution to the out-of-plane flexibility of the belt-rib. The spokes' configuration also defined the behaviour of the aerofoil, i.e. a morphing capability limited to the trailing edge. The structure was actuated via Bowden cables, and a spindle mechanism could deform the aerofoil section by  $\pm 5^\circ$ . A full-scale prototype was tested and withstood 335 kg in a static test. The advantages of this concept are numerous: integral compliant structure, a smooth aerofoil surface is achieved, wear and backlash are absent, maintenance is reduced, and safety is increased through structural redundancy. However, these attributes need to be considered against higher manufacturing complexity and uncertain fatigue performance.

In the concept presented by Wildschek *et al.*,<sup>83</sup> the trailing edge flap structure consisted of two outer skins stiffened with stringers and two inner middle skins able to slide relative to each other (Figure 30(a),(b)). By pushing/pulling the inner skins independently, the trailing edge could achieve different positions for roll and pitch control of the aircraft, or when both inner skins are pushed, the 'crocodile' shape was obtained for air braking. Wind tunnel tests demonstrated that the concept could withstand aerodynamic loads under high deflections. However actuation forces reached up to  $30 \text{ kN m}^{-1}$  span. Operational frequency was not disclosed in the article although it is believed that the frequency of actuation of the system would only be actuator dependant, as little inertia is associated with the flap structure itself.

Diaconu *et al.* investigated the use of bistable composite laminates to offer two trailing edge positions.<sup>43</sup> In this design, the deflection was achieved by inserting a square bistable composite laminate into the aerofoil section in a horizontal position along its chord, as shown in Figure 31. The leading edge of the bistable composite plate was clamped at its centre to the spar of the aerofoil section. The trailing edge of the plate was hinged to a vertical web, which was also hinged to the aerofoil surfaces to allow relative movement of the skins during actuation. At the aerofoil trailing edge, a discontinuity allowed the top skin to slide over the bottom skin during actuation. As the bistable plate snapped from one stable configuration to the other, deflection was induced at the trailing edge. Resistance of the structure against aerodynamic loads was not covered in the article. The use of a bistable plate reduced actuation cost, as power was only needed to switch the trailing edge from one position to the other; however, intermediate configurations of the trailing edge for fine aerodynamic adjustments were not possible.

Daynes *et al.* also used bistable composite laminates to obtain two trailing edge positions on a helicopter blade.<sup>37</sup> In this design, a series of bistable square laminates were inserted horizontally in the trailing edge section of the aerofoil, as

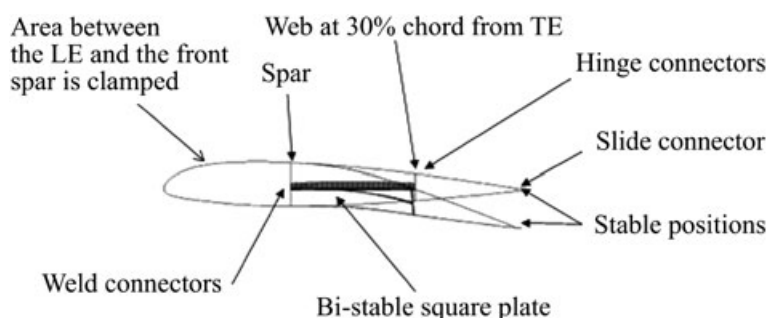


**Figure 31.** Morphing trailing edge using bistable composite plate.<sup>43</sup> LE, leading edge; TE, trailing edge.

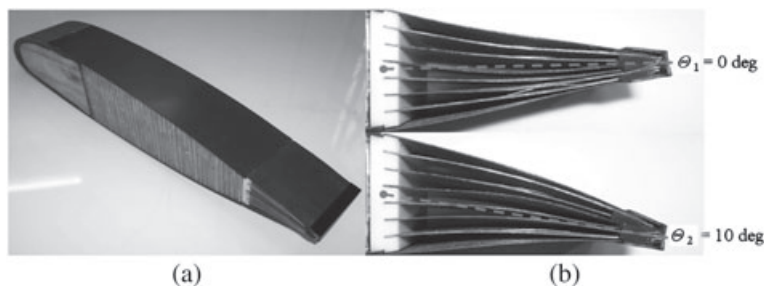


**Figure 32.** (a) Rotor blade section with bistable deformable trailing edge. (b) Trailing edge flap shown in the two stable positions.<sup>37</sup>

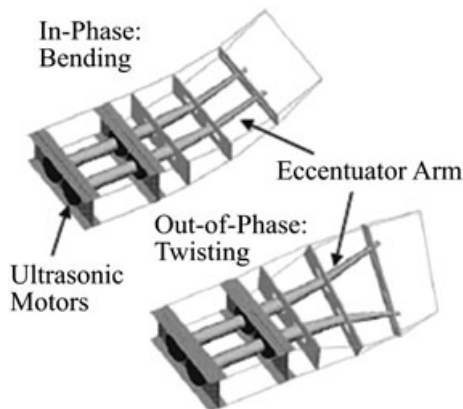


**Figure 33.** Morphing trailing edge using the eccentuator concept.<sup>31</sup>

shown in Figure 32(b). The morphing structure could deflect  $10^\circ$  down in 0.05 s induced by an electromechanical actuator mounted in the leading edge D-spar. Wind tunnel experiments showed that aerodynamic loads at  $60 \text{ m s}^{-1}$  were withstood without the help of any locking mechanism.<sup>84</sup>

The Smart Wing programme addresses the development of smart technologies and demonstration of relevant concepts to improve the aerodynamic performance of military aircraft under the initiative of the Smart Materials and Structures department of the Defense Advanced Research Projects Agency (DARPA).<sup>85</sup> One of the concepts in the Smart Wing programme consisted of a trailing edge sectioned into several segments, where each segment could undergo out-of-plane deformation by means of an eccentuator, as explained by Bartley-Cho *et al.*<sup>31</sup> The eccentuator concept is a bent beam that converts a rotary input at one end into a lateral and vertical translation at its other end. The vertical motion is used to morph the trailing edge, whereas the lateral motion is eliminated using sliding joints. The compliant trailing edge was designed using a central fibre glass laminate to provide sufficient out-of-plane stiffness to resist aerodynamic loads, whereas a flexible silicone skin was used to reduce actuation requirements. A honeycomb core provided flexibility and load transfer capability between the skin and the central laminate at any trailing edge position. A detailed picture of the structure is shown in Figure 5. Figure 33 shows the combination of two eccentulators for the twisting and bending of a trailing edge section. For the wind tunnel experiments, the morphing flap could achieve  $20^\circ$  of deflection in less than 0.33 s.

Daynes and Weaver<sup>32</sup> used a similar honeycomb structure for a morphing flap. The flap, designed for a wind turbine application, could morph  $\pm 15^\circ$  under loading. An aeroelastic analysis of the flap was performed, and the requirements for compliance, strength and reduced actuation cost were addressed. The flap demonstrator manufactured was 260 mm long in the chord-wise direction and 200 mm wide; its maximum thickness was 66 mm at its interface with the aerofoil structure. Actuation was achieved using a servo motor pushing/pulling a rod attached to the trailing edge of the flap and running through local CFRP guides on the pressure side, as illustrated in Figure 34. The next development phase of this project is wind tunnel testing to validate aerodynamic efficiency and fatigue testing.

In Strelec *et al.*,<sup>86</sup> SMA wires have been used to change the profile of a wing, a picture of the prototype is shown in Figure 35. The location of the SMA wires within the aerofoil section was optimised using a coupled finite element analysis and computational fluid dynamics environment. The thermomechanical response of the SMA actuators was also incorporated to simulate the structural response of the reconfigurable wing. A model wing was fabricated on the basis of the design

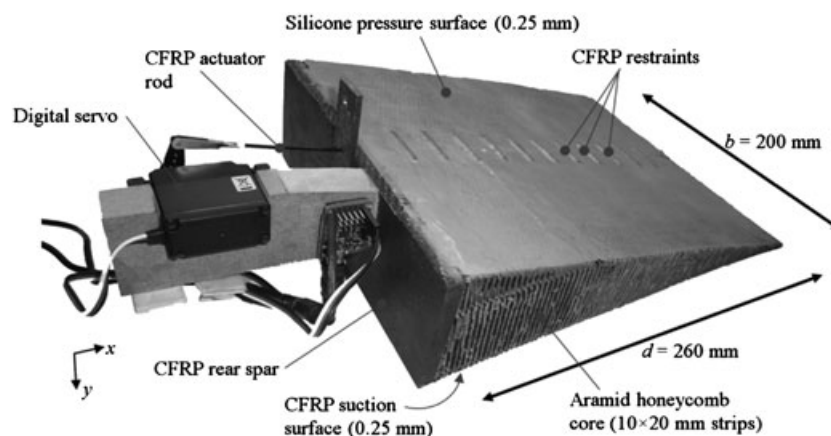


**Figure 34.** Wind turbine flap using a combination of carbon fibre reinforced polymer (CFRP) skin and honeycomb.<sup>32</sup>

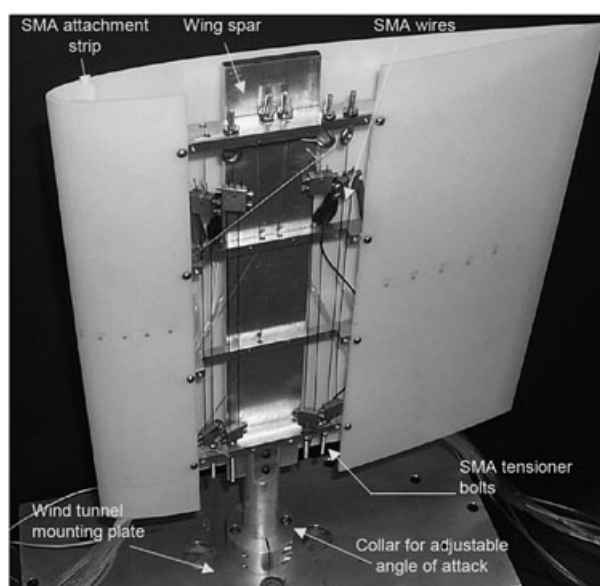


**Figure 35.** Shape memory alloy (SMA) wires were used by Strelec *et al.* to reconfigure the camber of their prototype wing.<sup>86</sup>

optimization to verify the predicted structural and aerodynamic response. Wind tunnel tests indicated an increase in lift for a given flow velocity and angle of attack by activating the SMA wire actuators. The pressure data taken during the wind tunnel tests followed the trends expected from the numerical pressure results. As highlighted by Lindroos,<sup>71</sup> the use of SMA wires could be a limiting factor for a wind turbine application, as the thermal inertia associated with the heating/cooling down cycles could restrict the operational frequency of the system.

In Coutu *et al.*,<sup>87</sup> discrete actuators positioned along the chord in a wing box and applied vertical displacements on the upper skin have been used to adjust the aerofoil profile and achieve camber change. The CFRP composite skin was clamped at the leading edge and attached to the trailing edge via a sliding plane link including a compensation spring placed between the flexible and rigid parts, as shown in Figure 36. However, this type of design suffered from weight penalties and structural complexity.

#### 4.2.3. Twist.

Another approach to morphing is to actively twist the entire blade along its span, as reported by Chopra<sup>16</sup> and Barlas and van Kuik,<sup>21</sup> resulting in a continuous variation of the angle of attack of the aerofoil along the blade length. Consequently, the change in angle of attack is larger at the blade tip, which is more effective for aerodynamic control. However,

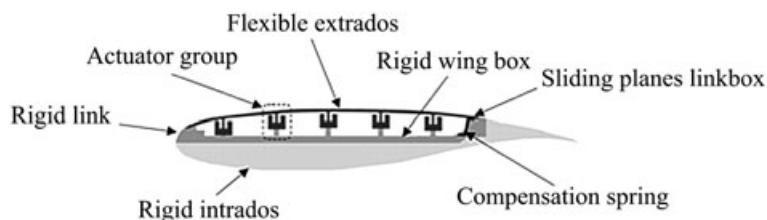


Figure 36. Camber morphing using discrete actuators.<sup>87</sup>

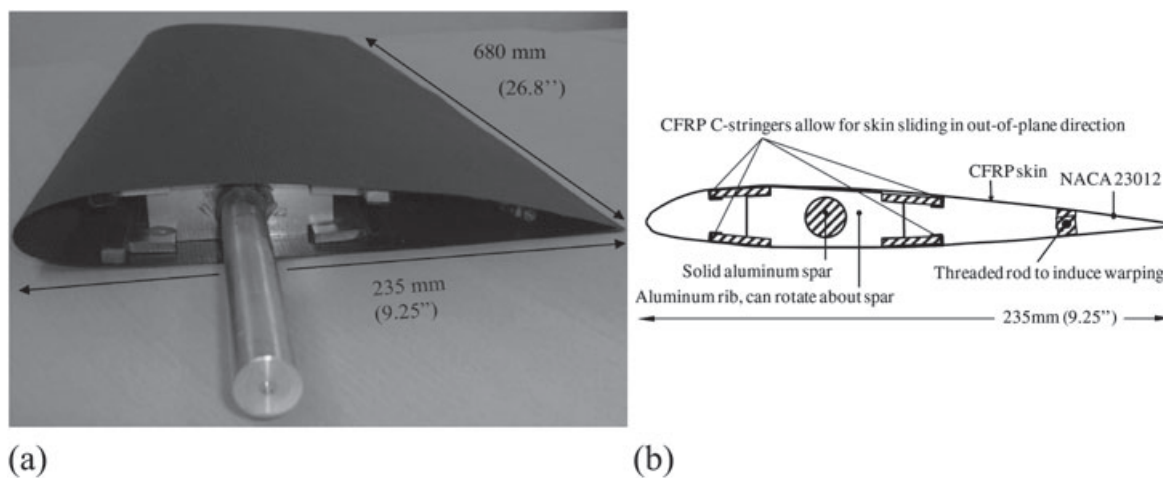
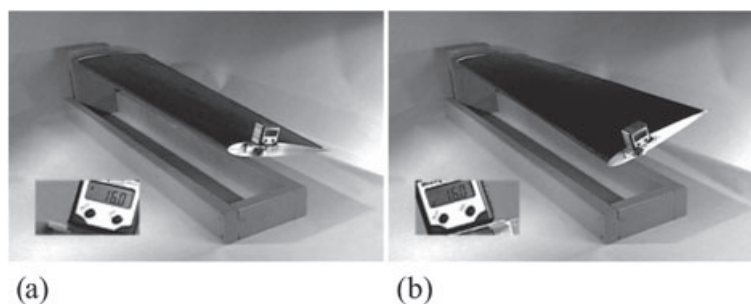


Figure 37. (a) Warp controlled morphing wing. (b) Schematic side view of the concept proposed by Vos *et al.*<sup>88</sup> CFRP, carbon fibre reinforced polymer.

no distributed control is possible over the span of the blade with this concept. To achieve such a twist, one concept is based on the active control of the bending–torsion or tension–torsion coupling of composite materials. For this, actuators are integrated within the blade made of anisotropic material. Research carried out for noise and vibration reduction in the rotorcraft industry showed aerodynamic control improvements, as detailed by Chopra.<sup>16</sup> Because of the large inertia of the wind turbine blade, response times were considered not fast enough, and actuation forces would be prohibitive to twist a whole blade according to Marrant and Van Holten.<sup>72</sup> The other inherent problem with active blade twist is that the complete blade must be made with active fibre composites. Because of the large amount of piezoelectric materials, cost would also become prohibitive. It could also lead to an increase in blade weight since lead is a common component in piezoelectric materials. Although small deflections can be obtained with this design, the blade must be torsionally compliant, which can be critically important with respect to flutter. One advantage of active twist is the smooth variation of the blade angle of attack, which does not change the aerodynamic behaviour of the original aerofoil design.

A recent experiment used the warping of an aerofoil skin to introduce the twist motion of the entire wing, as demonstrated by Vos *et al.*<sup>88</sup> In this design, the ribs were allowed to rotate freely around an aluminium rod serving as a main spar, and the skin was free to slide on the ribs in the span-wise direction, as illustrated in Figure 37. The CFRP wing skin was continuous over the surface of the aerofoil apart from the trailing edge, where the upper and lower skins were discontinuous. Warping was generated by creating a relative span-wise motion between the upper and lower skins at the trailing edge using a threaded rod running throughout the wing span. At several stations, nuts were fixed to the upper skin, whereas guidance was provided to the threaded rod on the lower skin. As a consequence, when the threaded rod was rotated, the upper and lower skins slide with respect to each other and twisting was introduced. Wind tunnel tests showed a change in the coefficient of lift of as much as 0.7 for angles of attack ranging from 0° to 12° and a peak to peak twist angle of 27° on a 0.68 m span wing. Adaptation to a wind turbine is yet to be demonstrated, but this promising concept allows large twist deformations of the aerofoil without affecting the aerodynamic profile of the blade. The operational frequency could be an issue if the device was employed against high-frequency phenomena.

Warp-induced twist was also investigated for a helicopter blade concept by Mistry *et al.*<sup>89</sup> In this parametric study, the influence of several parameters on the required actuation was assessed: blade span length, skin thickness, rib spacing and actuator nut spacing were considered. A finite element model, based on the built prototype shown in Figure 38, was



**Figure 38.** Prototype used for the parametric study by Mistry *et al.* in two twisted states: (a)  $+16^\circ$  and (b)  $-16^\circ$ .<sup>89</sup>

developed and used in conjunction with an analytical model to predict the behaviour of the structure while varying the parameters. A qualitative assessment was made, and it was reported that tip twist was more sensitive to span length than to skin thickness, whereas rib and actuator nut spacing had only a moderate effect. Actuation torque was reported to be highly sensitive to span length, skin thickness and actuator nut spacing, whereas rib spacing had a low influence. The study was made under no external loads, and the need for further study including operational loads to fully understand the structure kinematics was highlighted by Mistry. This concept was developed to enhance the performances of helicopters and tiltrotor aircrafts when switching from the hover mode to the high-speed forward flight mode; hence, the operational frequency was assumed very low.

## 5. CONCLUSIONS

With the growth in size of wind turbine blades, it has become difficult to rely upon passive power control, as was the case in the past, leading modern wind turbines to use sophisticated control systems, ensuring both safe and optimal operating conditions under a variety of atmospheric conditions. To enable further growth in size, wind turbines require yet another advance in load control. As larger rotors experience more pronounced structural and fatigue loading, particularly in turbulent winds, shape morphing brings possible structural solutions. The load reduction potential has already been shown in helicopters, where numerous concepts and experiments have been carried out. In the wind turbine area, numerical simulations and prototypes demonstrated the benefits of blade morphing. Aircraft wing morphing also provides a rich source of morphing concepts, although the level of load alleviation brought by concepts such as sweep morphing or span-wise bending needs to be evaluated and their adaptation to wind turbine blades might lead to complex structures. Because of their potentially high aerodynamic efficiency, simple construction and low weight, research in the wind turbine community focuses mainly on trailing edge flaps; however, span-wise or chord-wise expansion as well as twist morphing might also bring technical solutions to load reduction. Keeping in mind cost, simplicity and safety factors, the next phase in the development of large wind turbines is the integration of these compliant structures into the blade design, ensuring a better energy capture while increasing the turbine life.

## ACKNOWLEDGEMENTS

This work was supported by Vestas Wind Systems.

## REFERENCES

1. Hansen MOL. *Aerodynamics of Wind Turbines* 2nd edn. Earthscan: London, 2008.
2. Buhl T, Bak C, Gaunaa M, Andersen PB. Load alleviation through adaptive trailing edge control surfaces: ADAPWING overview, *European Wind Energy Conference & Exhibition (EWEC)*, Milan, Italy, 7-10 May 2007.
3. Zayas JR, van Dam CP, Chow R, Baker JP, Mayda EA. Active aerodynamic load control for wind turbine blades, *European Wind Energy Conference & Exhibition (EWEC)*, Athens, Greece, 27 February - 2 March 2006.
4. Bak C, Gaunaa M, Andersen PB, Buhl T, Hansen P, Clemmensen K, Moeller R. Wind tunnel test on wind turbine airfoil with adaptive trailing edge geometry, *45th AIAA Aerospace Sciences Meeting and Exhibit*, Reno, Nevada, USA, 8-11 January 2007.

5. Wilson DG, Berg DE, Barone MF, Berg JC, Resor BR, Lobitz DW. Active aerodynamic blade control design for load reduction on large wind turbines, *European Wind Energy Conference & Exhibition (EWEC)*, Marseille, France, 16–19 March 2009.
6. Andersen PB, Gaunaa M, Bak C, Buhl T. Load alleviation on wind turbine blades using variable airfoil geometry, *European Wind Energy Conference & Exhibition (EWEC)*, 27 February - 2 March 2006.
7. Bak C, Gaunaa M, Buhl T, Hansen P, Clemmensen K. Wind tunnel test on airfoil Risø-B1-18 with an active trailing edge flap. *Wind Energy* 2009; **13**: 207–219. DOI: 10.1002/we.369.
8. Lobitz DW, Veers PS, Bir G. Aeroelastic tailoring in wind-turbine blade applications, *Windpower '98*, Bakersfield, CA, USA, 27 Apr - 1 May 1998.
9. Lobitz DW, Veers PS. Aeroelastic behavior of twist-coupled HAWT blades, *Proceedings of Aerospace Sciences Meeting and Exhibit, 36th, and 1998 ASME Wind Energy Symposium*, Reno, Nevada, USA, 12-15 January 1998.
10. Lobitz DW, Veers PS, Eisler GR, Laino DJ, Migliore PG, Bir G. *The use of twist-coupled blades to enhance the performance of horizontal axis wind turbines*. Sandia National Labs: Albuquerque, New Mexico, USA, 2001. SAND2001-1303.
11. Ashwill TD, Kanaby G, Jackson K, Zuteck M. Development of the sweep-twist adaptive rotor (STAR) blade, *51st AIAA/ASME/ASCE/AHS/ASC Structures, Structural Dynamics & Materials Conference*, Orlando, Florida, USA, 4-7 January 2010.
12. Ashwill TD. Passive load control for large wind turbines, *51st AIAA/ASME/ASCE/AHS/ASC Structures, Structural Dynamics & Materials Conference*, Orlando, Florida, USA, 12-15 April 2010.
13. Ashwill TD, Albuquerque N, Veers PS, Griffin D, Locke J, Contreras I, Zuteck MD. Concepts for adaptive wind turbine blades, *40th AIAA Aerospace Sciences Meeting and Exhibit, ASME Wind Energy Symposium*, Reno, Nevada, USA, 14-17 January 2002.
14. Zuteck M. *Adaptive blade concept assessment: curved planform induced twist investigation*. Sandia National Laboratories: Clear Lake Shore, Texas, USA, 2002. SAND2002-2996.
15. Straub FK. A feasibility study of using smart materials for rotor control. *Smart Materials and Structures* 1996; **5**: 1–10. DOI: 10.1088/0964-1726/5/1/002.
16. Chopra I. Review of state of art of smart structures and integrated systems. *AIAA journal* 2002; **40**: 2145–2187. DOI: 10.2514/2.1561.
17. Hulskamp A. *Inventory of actuators and first order evaluation of 2 actuators and structural concepts*. Delft University of Technology: Delft, The Netherlands, 2007. Upwind Work Package 1B3, deliverable 3.
18. Thill C, Etches JA, Bond IP, Potter KD, Weaver PM. Morphing skins. *The Aeronautical Journal* 2008; **112**: 117–139.
19. Dieterich O, Enenkl B, Roth D. Trailing edge flaps for active rotor control-aeroelastic characteristics of the ADASYS rotor system, *American Helicopter Society 62nd Annual Forum*, Phoenix, AZ, USA, 9-11 May 2006.
20. Roth D, Enenkl B, Dietrich O. Active rotor control by flaps for vibration reduction—full scale demonstrator and first flight test results, *32nd European Rotorcraft Forum ERF 2006*, Maastricht, The Netherlands, 12-14 September 2006.
21. Barlas TK, van Kuik GAM. Review of state of the art in smart rotor control research for wind turbines. *Progress in Aerospace Sciences* 2010; **46**: 1–27. DOI: 10.1016/j.paerosci.2009.08.002.
22. Campanile LF. *Adaptive structures: engineering applications* (Wagg D, Bond IP, Weaver P, Friswell MI, eds). Wiley: Chichester, 2007. Chapter 4; Lightweight shape-adaptable airfoils: A new challenge for an old dream, p. 97.
23. Kikuta M. *Mechanical properties of candidate materials for morphing wings*, MSc Thesis, Mechanical Engineering, Virginia Polytechnic Institute and State University, 2003.
24. Peel LD, Jensen DW. The response of fiber-reinforced elastomers under simple tension. *Journal of Composite Materials* 2001; **35**: 96–137. DOI: 10.1106/V3YU-JR4G-MKJG-3VMF.
25. Peel LD, Jensen DW, Suzumori K. Batch fabrication of fiber-reinforced elastomer prepreg. *Journal of Advanced Materials* 1998; **30**: 3–10.
26. Gandhi F, Anusonti-Inthra P. Skin design studies for variable camber morphing airfoils. *Smart Materials and Structures* 2008; **17**: 1–9. DOI: 10.1088/0964-1726/17/01/015025.
27. Murray G, Gandhi F, Bakis C. Flexible Matrix composite skins for one-dimensional wing morphing. *Journal of Intelligent Material Systems and Structures* 2010; **21**: 1771–1781. DOI: 10.1177/1045389X10369719.
28. Olympio KR, Gandhi F. Zero-cellular honeycomb flexible skins for one-dimensional wing morphing, *48th AIAA/ASME/ASCE/AHS/ASC Structures, Structural Dynamics & Materials Conference*, Honolulu, Hawaii, USA, 23-26 April 2007.

29. Olympio KR, Gandhi F. Flexible skins for morphing aircraft using cellular honeycomb cores. *Journal of Intelligent Material Systems and Structures* 2009; **21**: 1719–1735. DOI: 10.1177/1045389X09350331.
30. Hexcel. *HexWeb® aluminium flex-core®—formable aluminium honeycomb data sheet*, 2006.
31. Bartley-Cho JD, Wang DP, Martin CA, Kudva JN, West MN. Development of high-rate, adaptive trailing edge control surface for the smart wing phase 2 wind tunnel model. *Journal of Intelligent Material Systems and Structures* 2004; **15**: 279–291. DOI: 10.1177/1045389X04042798.
32. Daynes S, Weaver PM. A shape adaptive airfoil for a wind turbine blade, *SPIE Smart Structures/NDE*, San Diego, California, USA, 6–10 March 2011.
33. Yokozeki T, Takeda S, Ogasawara T, Ishikawa T. Mechanical properties of corrugated composites for candidate materials of flexible wing structures. *Composites Part A: Applied Science and Manufacturing* 2006; **37**: 1578–1586. DOI: 10.1016/j.compositesa.2005.10.015.
34. Thill C, Etches JA, Bond IP, Potter KD, Weaver PM. Corrugated composite structures for aircraft morphing skin applications, *18th International Conference of Adaptive Structures and Technologies*, Ottawa, Ontario, Canada, 3–5 October 2007.
35. Thill C, Etches JA, Bond IP, Potter KD, Weaver PM, Wisnom MR. Investigation of trapezoidal corrugated aramid/epoxy laminates under large tensile displacements transverse to the corrugation direction. *Composites Part A: Applied Science and Manufacturing* 2010; **41**: 169–176. DOI: 10.1016/j.compositesa.2009.10.004.
36. Ge R, Wang B, Mou C, Zhou Y. Deformation characteristics of corrugated composites for morphing wings. *Frontiers of Mechanical Engineering in China* 2010; **5**: 73–78. DOI: 10.1007/s11465-009-0063-4.
37. Daynes S, Weaver PM, Potter KD. Aeroelastic study of bistable composite airfoils. *Journal of Aircraft* 2009; **46**: 2169–2173. DOI: 10.2514/1.44287.
38. Schultz MR. A concept for airfoil-like active bistable twisting structures. *Journal of Intelligent Material Systems and Structures* 2008; **19**: 157–169. DOI: 10.1177/1045389X06073988.
39. Guest SD, Pellegrino S. Analytical models for bistable cylindrical shells. *Proceedings of the Royal Society A: Mathematical, Physical and Engineering Science* 2006; **462**: 839–854. DOI: 10.1098/rspa.2005.1598.
40. Dano ML, Hyer MW. Thermally-induced deformation behavior of unsymmetric laminates. *International Journal of Solids and Structures* 1998; **35**: 2101–2120. DOI: 10.1016/S0020-7683(97)00167-4.
41. Seffen KA. ‘Morphing’ bistable orthotropic elliptical shallow shells. *Proceedings of the Royal Society A: Mathematical, Physical and Engineering Science* 2007; **463**: 67–83. DOI: 10.1098/rspa.2006.1750.
42. Daynes S, Potter KD, Weaver PM. Bistable prestressed buckled laminates. *Composites Science and Technology* 2008; **68**: 3431–3437. DOI: 10.1016/j.compscitech.2008.09.036.
43. Diaconu CG, Weaver PM, Mattioni F. Concepts for morphing airfoil sections using bi-stable laminated composite structures. *Thin-Walled Structures* 2008; **46**: 689–701. DOI: 10.1016/j.tws.2007.11.002.
44. Mattioni F, Weaver PM, Potter K, Friswell MI. Multi-stable composites application concept for morphing aircraft, *Proceedings of 16th International Conference of Adaptive Structures and Technologies*, Paris, France, 9–12 October 2005.
45. Potter K, Weaver P, Seman AA, Shah S. Phenomena in the bifurcation of unsymmetric composite plates. *Composites Part A: Applied Science and Manufacturing* 2007; **38**: 100–106. DOI: 10.1016/j.compositesa.2006.01.017.
46. Potter KD, Weaver PM. A concept for the generation of out-of-plane distortion from tailored FRP laminates. *Composites Part A: Applied Science and Manufacturing* 2004; **35**: 1353–1361. DOI: 10.1016/j.compositesa.2004.06.022.
47. ABAQUS/CAE. Simulia, 2008. <http://www.simulia.com/>.
48. Varelis D, Saravanos DA. Non-linear coupled multi-field mechanics and finite element for active multi-stable thermal piezoelectric shells. *International Journal for Numerical Methods in Engineering* 2008; **76**: 84–107. DOI: 10.1002/nme.2321.
49. Iqbal K, Pellegrino S. Bi-stable composite shells, *41st AIAA/ASME/ASCE/AHS/ASC Structures, Structural Dynamics, and Materials Conference and Exhibit*, Atlanta, GA, USA, 3–6 April 2000.
50. Guest SD, Kebabze E, Pellegrino S. A zero-stiffness elastic shell structure. *Journal of the Mechanics of Materials and Structures* 2011; **6**: 203–212.
51. Hahn B, Durstewitz M, Rohrig K. Reliability of wind turbines, *Proceedings of Euromech Colloquium*, Oldenburg, Germany, 4–7 October 2005. DOI:10.1007/978-3-540-33866-6\_62.
52. Neal DA, Good MG, Johnston CO, Robertshaw HH, Mason WH, Inman DJ. Design and wind-tunnel analysis of a fully adaptive aircraft configuration, *45th AIAA/ASME/ASCE/AHS/ASC Structures, Structural Dynamics & Materials Conference*, Palm Springs, California, USA, 19–22 April 2004.

53. Blondeau J, Richeson J, Pines DJ. Design, development and testing of a morphing aspect ratio wing using an inflatable telescopic spar, *44th AIAA/ASME/ASCE/AHS/ASC Structures, Structural Dynamics, and Materials Conference*, Norfolk, Virginia, USA, 7-10 April 2003.
54. Johnson SJ, van Dam CP, Berg DE. *Active Load Control Techniques for Wind Turbines*. Sandia National Laboratories: Albuquerque, New Mexico; Livermore, California, August 2008. SAND2008-4809.
55. Bubert EA. *Highly extensible skin for a variable wing-span morphing aircraft utilizing pneumatic artificial muscle actuation*, Msc Thesis, Aerospace Engineering, University of Maryland, 2009.
56. Perkins DA, Reed JL, Havens E. Morphing wing structures for loitering air vehicles, *45th AIAA/ASME/ASCE/AHS/ASC Structures, Structural Dynamics & Materials Conference*, Palm Springs, California, USA, 19-22 April 2004.
57. Reed Jr JL, Hemmelgarn CD, Pelley BM, Havens E. Adaptive wing structures, *Proceedings of Smart Structures and Materials 2005: Industrial and Commercial Applications*, San Diego, CA, USA, May 2005. DOI: 10.1117/12.599922.
58. Perkins DA, Reed JL, Havens E. Adaptive wing structures, *Proceedings of Smart Structures and Materials 2004: Industrial and Commercial Applications*, San Diego, CA, USA, 16 March 2004. DOI:10.1117/12.541650.
59. Flanagan JS, Stutzenberg RC, Myers RB, Rodrian JE. Development and flight testing of a morphing aircraft, the NextGen MFX-1, *48th AIAA/ASME/ASCE/AHS/ASC Structures, Structural Dynamics & Materials Conference*, Honolulu, Hawaii, US, 23-26 April 2007.
60. Joo JJ, Sanders B. Optimal Location of distributed actuators within an in-plane multi-cell morphing mechanism. *Journal of intelligent material systems and structures* 2009; **20**: 481.
61. Mattioni F, Weaver PM, Potter KD, Friswell MI. The application of thermally induced multistable composites to morphing aircraft structures, *Proceedings of Industrial and Commercial Applications of Smart Structures Technologies 2008*, 10 March 2008. DOI:10.1117/12.776226.
62. Lazos BS. Biologically inspired fixed-wing configuration studies. *Journal of Aircraft* 2005; **42**: 1089–1098. DOI: 10.2514/1.10496.
63. Wiggins LD, Stubbs MD, Johnston CO, Robertshaw HH, Reinholtz CF, Inman DJ. A design and analysis of a morphing hyper-elliptic cambered span (HECS) wing, *45th AIAA/ASME/ASCE/AHS/ASC Structures, Structural Dynamics & Materials Conference*, Palm Springs, California, USA, 19-22 April 2004.
64. Sofla AYN, Meguid SA, Tan KT, Yeo WK. Shape morphing of aircraft wing: status and challenges. *Materials and Design* 2010; **31**: 1284–1292. DOI: 10.1016/j.matdes.2009.09.011.
65. Migliore PG, Quandt GA, Miller LS. Wind turbine trailing edge aerodynamic brakes, *Windpower '95*, Washington, DC, USA, 27-30 March 1995.
66. Miller LS. *Experimental investigation of aerodynamic devices for wind turbine rotational speed control*. National Renewable Energy Lab: Golden, CO, USA, February 1995. Wichita State Univ., KS, USA.
67. Barlas TK, van Kuik GAM. Aeroelastic modelling and comparison of advanced active flap control concepts for load reduction on the Upwind 5MW wind turbine, *European Wind Energy Conference & Exhibition (EWEC)*, Marseille, France, 16-19 March 2009.
68. Barlas TK, van Wingerden JW, Hulskamp A, van Kuik G. Closed-loop control wind tunnel tests on an adaptive wind turbine blade for load reduction, *46th AIAA Aerospace Sciences Meeting and Exhibit*, 7-10 January 2008.
69. van Wingerden JW, Hulskamp AW, Barlas T, Marrant B, Van Kuik GAM, Molenaar DP, Verhaegen M. On the proof of concept of a 'smart' wind turbine rotor blade for load alleviation. *Wind Energy* 2008; **11**: 265–280. DOI: 10.1002/we.264.
70. UpWind. [Online]. Available: <http://www.upwind.eu/>. (Accessed 14 June 2011).
71. Lindroos T. *Adaptive wind turbine blade based on SMA composites*. VTT Technical Research Centre of Finland: Tmapere, Finland, 2009. Upwind Work Package 1B3, deliverable 11.
72. Marrant BAH, Van Holten T. Comparison of smart rotor blade concepts for large offshore wind turbines, *Offshore Wind Energy and Other Renewable Energies in Mediterranean and European Seas*, Rome, Italy, 20-22 April 2006.
73. Cadogan D, Smith T, Uhelsky F, MacKusick M. Morphing inflatable wing development for compact package unmanned aerial vehicles, *45th AIAA/ASME/ASCE/AHS/ASC Structures, Structural Dynamics & Materials Conference*, Palm Springs, California, USA, 19-22 April 2004.
74. Monner HP, Sachau D, Breitbach E. Design aspects of the elastic trailing edge for an adaptive wing. *Report ADP010488*, German Aerospace Center Braunschweig (Germany) Institute of Structural Mechanics, Braunschweig, Germany, 2000.
75. Poonsong P. *Design analysis of a multi-section variable camber wing*, MSc Thesis, Aerospace Engineering, University of Maryland, 2004.



76. Kota S. Compliant systems using monolithic mechanisms. *Smart Materials Bulletin* 2001; **2001**: 7–10. DOI: 10.1016/S1471-3918(01)80002-2.
77. Kota S, Hetrick J, Osborn R. Design and application of compliant mechanisms for morphing aircraft structures, *Proceedings of Smart Structures and Materials 2003: Industrial and Commercial Applications of Smart Structures Technologies*, San Diego, CA, USA, 4 March 2003.
78. Berg DE, Wilson DG, Resor BR, Barone MF, Berg JC, Kota S, Ervin G. *Active aerodynamic blade load control impacts on utility-scale wind turbines*. Sandia National Laboratories: Albuquerque, NM, USA, 2009.
79. Shili L, Wenjie G, Shujun L. Optimal design of compliant trailing edge for shape changing. *Chinese Journal of Aeronautics* 2008; **21**: 187–192. DOI: 10.1016/S1000-9361(08)60024-2.
80. Gandhi F, Frecker M, Nissly A. Design optimization of a controllable camber rotor airfoil. *AIAA journal* 2008; **46**: 142–153. DOI: 10.2514/1.24476.
81. Campanile LF, Sachau D. The belt-rib concept: a structronic approach to variable camber. *Journal of Intelligent Material Systems and Structures* 2000; **11**: 215–224. DOI: 10.1106/6H4B-HBW3-VDJ8-NB8A.
82. Campanile LF, Hanselka H. A lightweight concept for aerodynamic surfaces with variable camber, *21st ICAS Congress*, Melbourne, Australia, 13–18 September 1998.
83. Wildschek A, Havar T, Plötner K. An all-composite, all-electric, morphing trailing edge device for flight control on a blended-wing-body airliner. *Proceedings of the Institution of Mechanical Engineers, Part G: Journal of Aerospace Engineering* 2009; **224**: 1–9. DOI: 10.1243/09544100JAERO622.
84. Daynes S, Nall SJ, Weaver PM, Potter K, Margaris P, Mellor PH. Bistable composite flap for an airfoil. *Journal of Aircraft* 2010; **47**: 334–338. DOI: 10.2514/1.45389.
85. Kudva JN, Martin CA, Scherer LB, Jardine AP, McGowan AM, Lake RC, Sendekyj GP, Sanders BP. Overview of the DARPA/AFRL/NASA Smart Wing program, *Proceedings of Smart Structures and Materials 1999: Industrial and Commercial Applications of Smart Structures Technologies*, Newport Beach, CA, USA, 1999. DOI:10.1117/12.351561.
86. Strelec JK, Lagoudas DC, Khan MA, Yen J. Design and implementation of a shape memory alloy actuated reconfigurable airfoil. *Journal of Intelligent Material Systems and Structures* 2003; **14**: 257–273. DOI: 10.1177/1045389X03034687.
87. Coutu D, Brailovski V, Terriault P. Optimized design of an active extrados structure for an experimental morphing laminar wing. *Aerospace Science and Technology* 2010; **14**: 451–458. DOI: 10.1016/j.ast.2010.01.009.
88. Vos R, Gürdal Z, Abdalla M. Mechanism for warp-controlled twist of a morphing wing. *Journal of Aircraft* 2010; **47**: 450–457. DOI: 10.2514/1.39328.
89. Mistry M, Gandhi F, Nagelsmit M, Gurdal Z. Actuation requirements of a warp induced variable twist rotor blade. *Journal of Intelligent Material Systems and Structures* 2011; **22**: 919–933. DOI: 10.1177/1045389X11404957.